Doctoral Dissertation (Censored)

博士論文 (要約)

Paleoenvironmental reconstruction using geochemical and rock magnetic analyses for carbonates obtained from the Kingdom of Tonga, South Pacific

(地球化学・岩石磁気学的測定による南太平洋トンガ王国の古環境復元)

A Dissertation Submitted for the Degree of Doctor of Philosophy

December 2020

令和２年１２月博士（理学）申請

Department of Earth and Planetary Science, Graduate School of Science, The University of Tokyo

東京大学大学院理学系研究科

地球惑星科学専攻

Naoto Fukuyo

福與　直人

Acknowledgment

I am deeply grateful to all the people who provided support and advised me in completing my Ph.D. research; I would like to sincerely appreciate my supervisor, Prof. Yusuke Yokoyama, who provided me so many opportunities from diverse aspects. I would like to express my greatest appreciation to Prof. Geoffrey Clark and Dr. Hirokuni Oda for the considerable supports, discussions, and advices on all aspects of my research. I would like to sincerely appreciate Dr. Yosuke Miyairi and Dr. Kaoru Kubota for their generous support of my research. Dr. Tomoko Bell kindly supported my first field sampling in Tonga. I would like to express my deep gratitude to Dr. Takahiro Aze and Dr. Chikako Sawada for radiocarbon measurements at Atmosphere and Ocean Research Institute (AORI). Dr. Anthony Purcell and Dr. Glenn Milne spent a lot of time to teach me how to use the GIA model. Mr. Philip Parton fully supported the reconstruction of the paleoshoreline. I greatly appreciated to Dr. Shirai and his laboratory members for the measurements of oxygen isotope ratios in bivalves at AORI. Dr. Miyajima taught me the measurements of oxygen isotope ratios in seawater at AORI. I am thankful to the late Mr. Nivarati Melekiola and Ms. Malia Melekiola for their supports on sampling in Tonga. I would like to express my gratitude to JSPS Fellows DC1 (JP18J21630) for their financial support.

I would like to express my most tremendous gratitude to my mother Noriko, and my sister Asuka, who provided plenty of support and patience to me during the Ph.D. course. Finally, I would like to express my most generous gratitude to my father, Takashi, for supporting my life. I hope his brain dysfunction improves someday and wish him to celebrate my thesis's completion.

Malo e lelei

Abstract

South Pacific islands are extremely vulnerable to environmental changes such as sea-level rise, storm surges, earthquakes, and volcanic eruptions. The changes increase the probability of forced migration in the future. Meanwhile, archaeological studies suggest that a comparable situation occurred in this region during the Middle and Late Holocene. Thus, there is an urgent need to understand the mechanisms, variability, and impacts of environmental changes. However, the limited availability of environmental observations of this region before the mid-twentieth century means that paleoenvironmental reconstructions from natural archives, such as bivalves and speleothems, offer valuable tools for reconstructing the past variability of environmental changes. However, few quantitative paleoenvironmental studies using geochemical or geophysical methods have been reported.

Here, I reconstructed the paleoenvironment in the Kingdom of Tonga (Tonga) using geochemical and rock-magnetic analyses for bivalves and speleothems with developing novel proxies. Tonga is one of the South Pacific island countries and was a source area for the peopling of East Polynesia around 1,000 years ago; thus, it is suitable for studying paleoenvironmental reconstruction in the South Pacific and its related human migration.

First, I examined live-caught and archaeological shells, *Gafrarium tumidum,* to establish a novel proxy for the ratio of the freshwater inlet to the lagoon water. As a result, I defined the lagoon-specific local marine reservoir ages (ΔR_{lagoon}) of prehistoric bivalves as an influx of old ^{14}C from terrestrial limestone. Then, I reconstructed Tongatapu Island's sea-level history using radiocarbon measurements and glacio-hydro-isostatic adjustment (GIA) modeling. Our analyses reconstructing the lagoon's evolution suggest that the average size of *G. tumidum* decreased synchronously with corresponding changes

in the paleoenvironment. These changes also correspond to the increasing trend of ΔR_{lagoon} from 105±49 to 156±85 years between ~2.6 and 1.2 ka. The decline in the shellfish assemblage within Fanga'uta Lagoon reported in previous studies was also synchronous with these changes, which were caused by a decrease in the exchange of water in and out of the lagoon. GIA modeling predicts mid-Holocene sea-level highstand (HHS) was less than 1 m above the present sea level in Tongatapu, suggesting that the previously reported observations of an HHS require additional contributions, perhaps from crustal uplift. Furthermore, recent Global Navigation Satellite System (GNSS) observations of vertical uplift rates at Tongatapu have a higher magnitude than the long-term uplift rate obtained from Holocene sea-level data.

Second, I applied a scanning SQUID microscopy (SSM) to conduct paleomagnetic measurements on a stalagmite collected from Anahulu Cave in Tonga. A stronger magnetic field was observed above the grayish surface layer compared to that of the white inner layer associated with the laminated structures of a speleothem at the submillimeter scale with the SSM. The magnetization of the speleothem sample calculated by an inversion of isothermal remanent magnetization (IRM) also suggests that the magnetic mineral content in the surface layer is higher than that in the inner layer. This feature was further investigated by low-temperature magnetometry and suggested that it contains magnetite, maghemite, and goethite. The first-order reversal curve (FORC) measurements and the decomposition of IRM curves show that this speleothem contains a mixture of magnetic minerals with different coercivities and domain states. The contribution from maghemite and goethite to the total magnetization of the grayish surface layer is much higher than for the white inner layer. The speleothem magnetically and visually retaining two distinct layers indicates that the depositional environment was

shifted when the surface layer was deposited and was likely changed due to an oxidative environment such as volcanic eruption or/and human activities.

Future investigation is required to reveal the detail of linking environmental changes (e.g., climate change and sea-level change) to human activities in the South Pacific, but I have helped initiate this by demonstrating the potential to reconstruct the paleoenvironment in the Kingdom of Tonga using geochemical analyses for *G. tumidum* and rock magnetic analyses for the speleothem.

Contents

Chapter 1. General Introduction 1

1.1. Human migration as a result of environmental changes in the Pacific islands 3

1.2. Case studies of environmental changes that island nations are facing 4

1.2.1 Climate change 4

1.2.2 Earthquake, tsunami, and volcanic eruption 5

1.3. Geological setting of Tonga 6

1.4. Archaeological studies in Tonga 7

1.5. Radiocarbon dating and Marine Reservoir effect 9

1.6. Speleothem magnetism 10

1.7. Research objective and thesis structure 12

Chapter 2. Development of novel proxy; lagoon-specific local marine reservoir effect –Application to Holocene sea level reconstruction with geophysical modeling in Tongatapu, Kingdom of Tonga– 17

Summary 19

2.1. Introduction 20

2.1.1. Holocene sea level change and glacio-hydro isostasy 20

2.1.2. Quantification of rheological parameters and geophysical activities using GIA model 23

2.1.3. The aim of this chapter 24

2.2. Materials and Methods 25

2.2.1. Site Description and Sample Collection 25

2.2.2. Sample collection and preparation 26
2.2.3. Stable oxygen isotope analyses 28
2.2.4. Radiocarbon dating 29
2.2.5. Calculation of lagoon-specific marine reservoir effect (ΔR_{lagoon}) 29
2.2.6. GIA modeling and shoreline reconstructions 31

2.3. Results 36

2.3.1. Modern seawater temperature and salinity measurements 36
2.3.2. $\delta^{18}O$ composition of seawater 38
2.3.3. Shell size of *G. tumidum* 41
2.3.4. $\delta^{18}O$ composition of shells 48
2.3.5. Radiocarbon measurements and ΔR_{lagoon} 51
2.3.6. GIA modeling 57

2.4. Discussion 59

2.4.1. The Relationship between $SSS_{in\ situ}$ and $\delta^{18}O_{sw}$ in Fanga' Uta lagoon 59
2.4.2. Relationship between $\delta^{18}O_{shell}$ and SST and $SSS_{in\ situ}$ in Fanga' Uta lagoon 61
2.4.3. Reconstruction of SSSs using fossil bivalves in Fanga' Uta lagoon and its limitation ... 64
2.4.4. Suitability of *G. tumidum* ^{14}C as a proxy for ΔR_{lagoon} 67
2.4.5. Holocene changes in lagoon water properties inferred from the ΔR_{lagoon} of *G. tumidum* 72
2.4.6. Paleotopographic reconstruction 74
2.4.7. Comparison of GIA modeling to sea level indicators and GNSS (GPS) observation ... 75
2.4.8. Comparison of previously reported sea level indicators with GIA predictions and ΔR_{lagoon} 78
2.4.9. Shell sizes related to paleoenvironmental changes 80

2.5. Conclusion 82

Chapter 3. High spatial resolution magnetic mapping using ultra-high sensitivity scanning SQUID microscopy on a speleothem from the Kingdom of Tonga, southern Pacific 83

Summary ····· **84**

3.1. Introduction ····· **87**

3.2. Methods ····· **90**

3.3. Results ····· **96**

3.3.1. Radiocarbon dating ····· 96

3.3.2. SSM measurements ····· 101

3.3.3. Magnetic mineralogy with low-temperature magnetometry ····· 107

3.3.4. Hysteresis and domain state diagnosis using FORC ····· 110

3.3.5. Identification of coercivity components using IRM acquisition curves ····· 112

3.4. Discussion ····· **114**

3.4.1. Timing of speleothem layers formation ····· 114

3.4.2. Sensitivity, reliability, and implications of SSM measurements ····· 115

3.4.3. Magnetic minerals in this speleothem ····· 116

3.4.4. Environmental magnetic implication ····· 118

3.5. Conclusion ····· **121**

Chapter 4. General conclusion and Future work ····· 123

4.1. General conclusion ····· **125**

4.2. Future perspectives ····· **127**

4.2.1. Linking environmental changes to human activities in the South Pacific ····· 127

4.2.2. Estimations of vertical land motion over different time scales ····· 128

4.2.3. The potential of speleothem as environmental proxies ····· 130

Reference ····· 132

Appendix 1: Trace element analyses ····· 149

Chapter 1. General Introduction

1.1. Human migration as a result of environmental changes in the Pacific islands

Throughout history, humans have been forced to migrate for various reasons, such as wars, disasters, and enslavements (Becker *et al.,* 2020; Cashman & Giordano 2008; Schroeder *et al.,* 2009). In the Pacific Islands, climate and sea-level changes have played a major role in human migration (e.g., Kayanne *et al.,* 2011; Nunn & Carson, 2015). For example, in Palau, ca. 1300 A.D., a comparatively rapid cooling likely caused the island group's abandonment (e.g., Clark & Reepmeyer 2012).

In modern times, most small Pacific Island countries are inherently vulnerable to environmental changes and highly exposed to natural hazards, and they will be increasingly vulnerable due to climate change (Chand 2020). Therefore, in terms of adaptation to environmental change in the present and future, it is important to understand the past environment's effect on human activities.

The Kingdom of Tonga is rated the second-greatest disaster-risk nation in the Pacific (Garschagen *et al.,* 2014). It was a source area for the migration to East Polynesia around 1,000 years ago (Clark *et al.,* 2015); thus, it is suitable for studying the paleoenvironment and its relation to human migration.

1.2. Case studies of environmental changes that island nations are facing

1.2.1 Climate change

Precipitation brought by the South Pacific Convergence Zone (SPCZ) significantly impacts South Pacific island countries such as Fiji and Tonga. For island countries vulnerable to climate change, accurate predictions of SPCZ changes are of great importance for the people's livelihoods and economic activities in the region. The Fifth Report of the Intergovernmental Panel on Climate Change (IPCC; Intergovernmental Panel on Climate Change, 2014) suggests that the SPCZ may move more northeastward and that precipitation in the South Pacific may decrease. However, current climate models are not very accurate in predicting the future of the tropical convergence zones, including the SPCZ (e.g., Brown *et al.,* 2020), and paleoclimate collection records are essential to understand the mechanisms and modes of change. Previous SPCZ studies have collected paleoclimatic records, including oxygen isotope analyses of in situ corals from Fiji and Tonga (Linsley *et al.,* 2006), which reconstruct past SPCZ fluctuations.

However, previous studies of SPCZ's paleoclimatic reconstructions in the South Pacific using in situ corals have been limited to the past 2–300 years, which is less than 1/10th of the El Niño Southern Oscillation (ENSO) and other mid- to low-latitude climate reconstructions.

1.2.2 Earthquake, tsunami, and volcanic eruption

Earthquakes and volcanic eruptions have repeatedly occurred near the Tonga Trench. Recently, an earthquake of Mw=7.9 occurred in 2006, and a tsunami caused by the earthquake was observed (e.g., Tang *et al.,* 2008). The following year, the Samoa-Tonga earthquake of Mw=8.1 (e.g., Lay *et al.,* 2010) and the eruption of the Hunga Ha'apai-Hunga Tonga volcano occurred in the territory of the Kingdom of Tonga (e.g., Bohnenstiehl *et al.,* 2013). Thus, Tonga is a region of repeated seismic and volcanic activity due to the subduction of the Pacific Plate. The earliest records of earthquakes and volcanic eruptions in this region are from 1853 (Sawkins, 1856) and 1774 (Cook, 1777), respectively. However, the start of subduction in this region is reported to be about 52–48 Ma (e.g., Meffre *et al.,* 2012), suggesting that the present subduction zone was formed and maintained with some changes since then. In other words, although earthquakes and volcanic eruptions occurred before the 18th century, it is difficult to reconstruct the history of these old earthquakes and volcanic activities using historical records. Therefore, to understand the prehistoric earthquakes and volcanic eruptions, it is necessary to reconstruct the activity history using geological records.

1.3. Geological setting of Tonga

The islands of Tonga are situated in the southwest Pacific, some 780 km east of Fiji, 900 km southwest of Samoa, and 2200 km northwest of New Zealand (Figure 1-1). They consist of 171 islands and lie from 15° to 23° 5' S and from 173° W to 177° W. The archipelago extends in an NNE-SSW direction and is commonly divided into four groups: the southern Tongatapu group, the Ha'apai group, the northern Vava'u group, and the northernmost Niues.

Tonga is located on the crest of the Tonga ridge parallel to the Tonga trench. Here the Pacific tectonic plate subducts beneath the Indo-Australian plate. The Kingdom of Tonga, therefore, lies in a geologically tectonically active area, and large earthquakes occur repeatedly. The plate subduction triggers arc magmatism that feeds volcanism along the active Tofua arc, which lies west of the Tongan islands. The geometry of the subducted Pacific slab beneath Tonga is complicated. Tomographic images suggest the subducting plate enters the upper mantle by lying flat, bending, or detaching under the Tonga Trench (e.g., Fukao & Obayashi, 2013; Tibi & Wiens, 2005; van der Hilst, 1995).

Tongatapu Island is an uplifted coral atoll. It is made up of Pliocene and Pleistocene limestone 150–250 m thick overlying lower Pliocene and older volcaniclastics (e.g., Cunningham & Anscombe, 1985; Taylor, 1978). Holocene deposits in Tongatapu include reef limestones and detrital sediments accumulated in the beach, tidal flat, and lagoonal environments (Figure 1–2).

1.4. Archaeological studies in Tonga

Tonga is also an archaeologically important region that was a hub for human migration to East Polynesia (Clark *et al.,* 2015). Goodwin *et al.* (2014) suggest that the diffusion of humans to the South Pacific Islands is thought to have been closely related to sea-level and climate changes. Tonga served as a hub for human dispersal to Eastern Polynesia, and it has been suggested that multi-decadal-scale changes may have influenced human migration routes in sea-level pressure and wind direction.

Based on the RSL records and the coarse-resolution topographic maps (2 m contour), the mid-Holocene paleoshoreline around Fanga ‘Uta Lagoon, Tongatapu island was reconstructed (e.g., Dickinson, 2007; Spennemann, 1997, see Figure 1-3). The modern Fanga ‘Uta lagoon is a shallow and restricted body of water and is largely closed from tidal influence. The water in the lagoon is brackish with a mean residence time of ca. 20 – 30 days (Damlamian 2008; Zann *et al.* 1984). In mid-Holocene time, extending at least until the first human occupation in Tongatapu, the lagoon was an open embayment. As sea level fell, the lagoon has become increasingly enclosed and shoaled, and salinity in the lagoon decreased, which would have had a large negative impact on the quality and quantity of benthic habitats (Burley *et al.,* 2001; Clark *et al.,* 2015; Spennemann 1987).

For example, Spennemann (1987) argued that *Anadara antiquata* in shell midden radically declined due to a radical change of the lagoon environment, which was caused by sea level fall. *A. antiquata* favors sandy and sometimes muddy substrates in intertidal reef flats of the near-shore environment and prefers saline conditions (Spennemann, 1989). Moreover, a small oyster, *Dendrostrea folium*, was the most abundant species in the Talasiu midden and had attached corals (e.g., Clark *et al.,* 2015). However, there are

no corals nor *D. folium* in modern Talasiu. These species can be found at the lagoon mouth only today (Zann, 1984)

However, the previous studies were based on the archaeological method, and no studies of quantitative paleoenvironmental studies using geochemical methods have been reported.

1.5. Radiocarbon dating and Marine Reservoir effect

Radiocarbon (^{14}C) is one of the most important dating tools used to reconstruct the timing of changes in Earth and human history over the past 50,000 years. The value of ^{14}C can be used in the traditional sense of assigning a calendar age to a historical event (Fukuyo *et al.,* 2019).

But it is also used as a tracer for processes, such as ocean circulation (Hirabayashi *et al.,* 2019; Kubota *et al.,* 2018). The marine surface mixed layer is depleted in radiocarbon relative to the atmosphere because of upwelling of radiocarbon-depleted deep water and slow mixing across the ocean-atmosphere interface. The difference between oceanic and atmospheric radiocarbon ages is defined as the Marine reservoir age (R) (Alves *et al.,* 2018; Hirabayashi *et al.,* 2019; Stuiver & Polach, 1977) and the averaged marine reservoir age of the surface ocean is ca. 400 years. However, local marine reservoir age offsets (ΔR) are induced by local environmental conditions (e.g., Hirabayashi *et al.,* 2017; Lindauer *et al.,* 2017a). In this study, I used ^{14}C values as change depending on the amount of freshwater input and marine incursion (See Chapter 2).

1.6. Speleothem magnetism

Conventional methods aimed to unveil the evolution of the geomagnetic field extract paleomagnetic signals recorded in geologic materials such as volcanic rocks and sediments. However, obtaining an accurate chronology from these geologic archives is not trivial. Age uncertainties from radiometric dating of volcanic rocks typically present age errors with a few percent (e.g., several hundreds of years for ~50 ka rock) that make it challenging to depict a precise picture of events. The age models of sediments are often indirect, and the magnetization of sediments lag behind by as much as thousands of years due to magnetization acquisition mechanisms called lock-in depth (Roberts *et al.,* 2013).

Recently, speleothems have been used to overcome these problems because they capture the geomagnetic signals synchronously with the formation of carbonate layers, incorporating magnetic minerals. Samples can be dated radiometrically using the Uranium-series dating method. Compared to sediments, their structures are not impacted by later diagenesis, consolidation, or deformation after the deposition. Moreover, the time lag between their crystallization and lock-in of paleomagnetic signals is fairly small (e.g., Latham *et al.,* 1979; Morinaga *et al.,* 1989), and several speleothem magnetism studies report accurate ages of geomagnetic excursions using U/Th-dated speleothems (e.g., Lascu *et al.,* 2016; Osete *et al.,* 2012; Pozzi *et al.,* 2019).

Another advantage of using speleothems to reconstruct paleomagnetism is that they can record the paleoenvironment using environmental magnetism methods (Lascu & Feinberg, 2011). Magnetic minerals deposited on speleothems are sourced from floodwaters, which flow into caves and/or produce drip action filtering in overlying soils. The magnetic minerals in speleothems can therefore record regional and global environmental changes such as paleofloods, precipitation, and anthropogenic influences

as variations in rock magnetic properties (e.g., Feinberg *et al.,* 2020; Font *et al.,* 2014; Jaqueto *et al.,* 2016). Despite the advantages mentioned above, the paleomagnetic signals of speleothems are too weak to reconstruct high-resolution paleomagnetic records using conventional magnetometers (Lascu *et al.,* 2016). Thus, previous studies had to sacrifice the temporal resolution that speleothems could potentially offer. The problem can be overcome using a scanning superconducting quantum interference device microscope (scanning SQUID microscopy) to a speleothem.

The SQUID microscope allows the scanning of samples of about 100 μm at room temperature. It can also detect dipole fields with moments that are weaker than 10 – 15 Am^2 making it more sensitive than the best superconducting moment magnetometers (Oda *et al.,* 2016). However, only two preliminary paleomagnetism studies have been reported using SSM for speleothems (Feinberg *et al.,* 2020; Myre *et al.,* 2019).

1.7. Research objective and thesis structure

As mentioned above, various paleoenvironmental changes have affected human activities, especially in the Pacific islands (e.g., Clark *et al.,* 2015; Clark & Reepmeyer 2012; Kayanne *et al.,* 2011; Nunn & Carson, 2015). Therefore, one of the effective ways to reconstruct each paleoenvironmental change is combining multiple proxies.

The main objective of this thesis to understand the paleoenvironment in the Kingdom of Tonga (Tonga) using bivalves and speleothems. To achieve this research objective, I examined new methods using geochemical and rock-magnetic analyses for bivalves and speleothems. In Chapter 2 (cf., Fukuyo *et al.,* 2020), I developed a new proxy for freshwater proportions in a lagoon and reconstructed sea level change during Holocene and its influence on the lagoon environment using this novel proxy, GIA models, and LiDAR data. In Chapter 3, I applied a scanning SQUID microscopy to a speleothem and interpreted variations in rock magnetic properties recorded in the speleothem. Lastly, the key findings of this thesis will be summarized, and future avenues for this research will be suggested (Chapter 4).

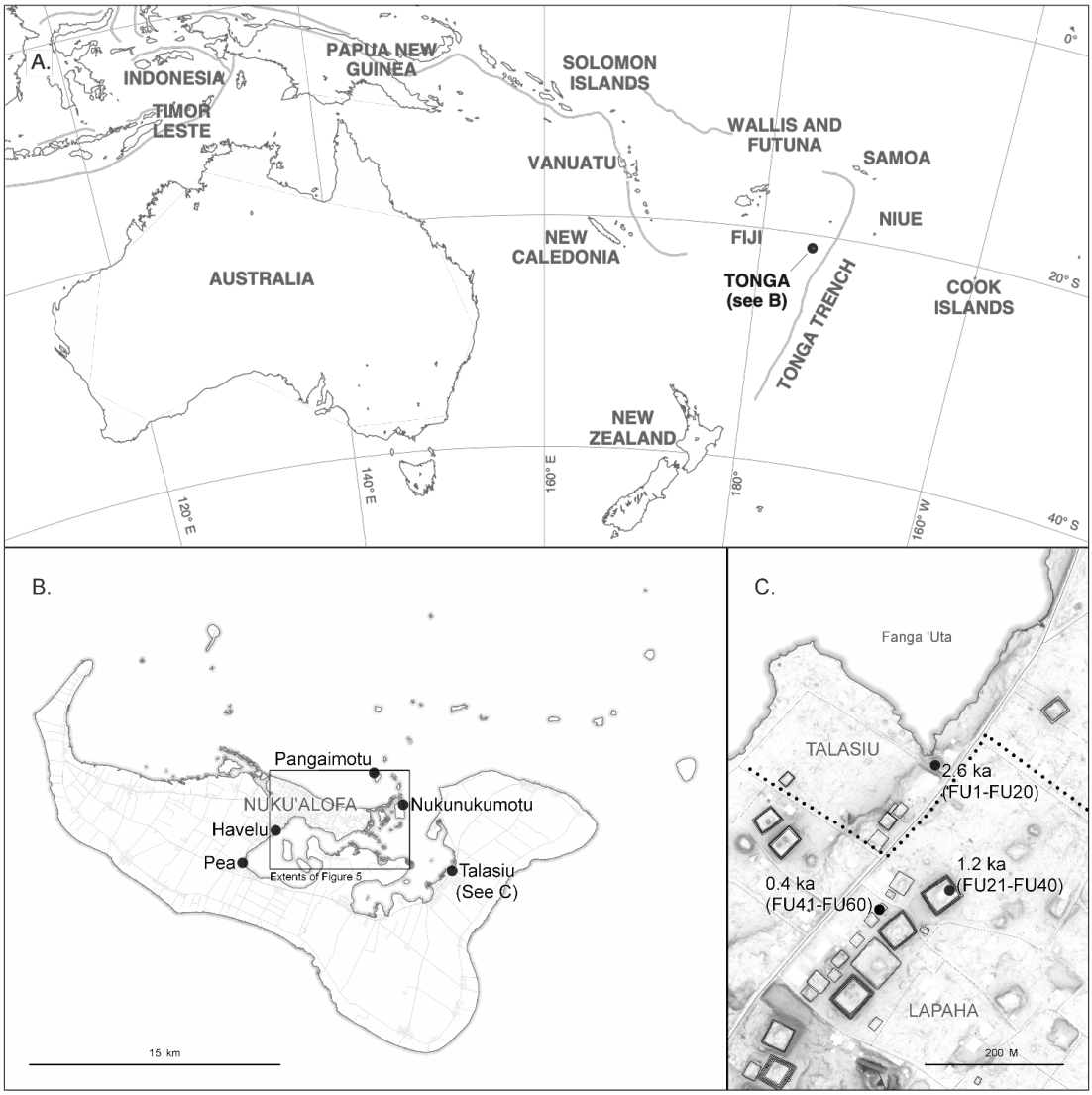

Figure 1-1. Sampling sites in this study. (A) The location of the Kingdom of Tonga. (B) Sampling sites on Tongatapu Island. Havelu and Pangaimotu are sites with shells of known ages reported in Spennemann & John Head (1998). The inset square indicates the extent of Figure 2-4. (C) Archaeological sites in Talasiu and Lapaha. The dashed line denotes the border between Talasiu and Lapaha. From Fukuyo *et al.* (2020).

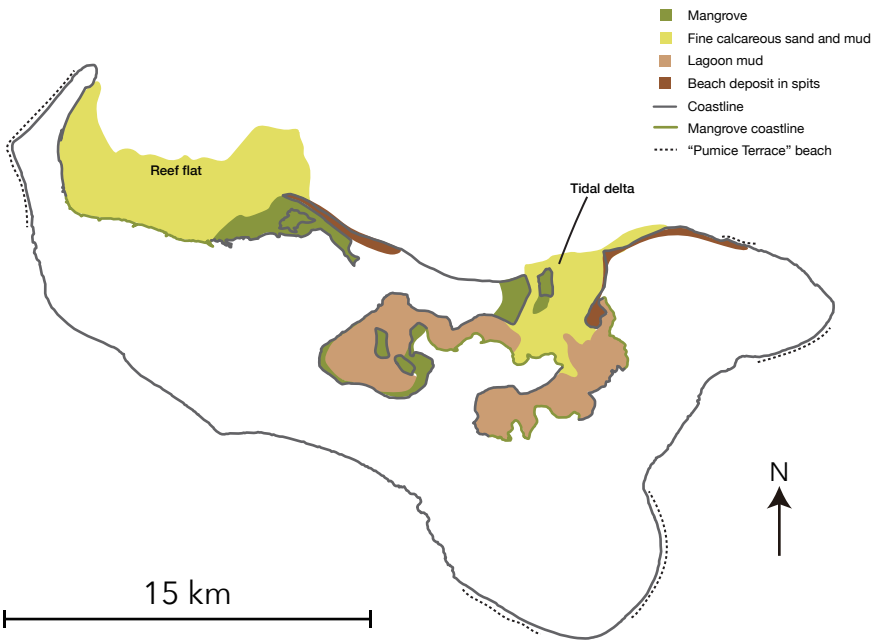

Figure 1-2 Tongatapu island, showing distribution of main Holocene depositional environments. Main land forms a surficial pavement characterised by Porities microatolls and Acropora fragments. The geological Information from Roy (1997) and van der Velde *et al.* (2006b).

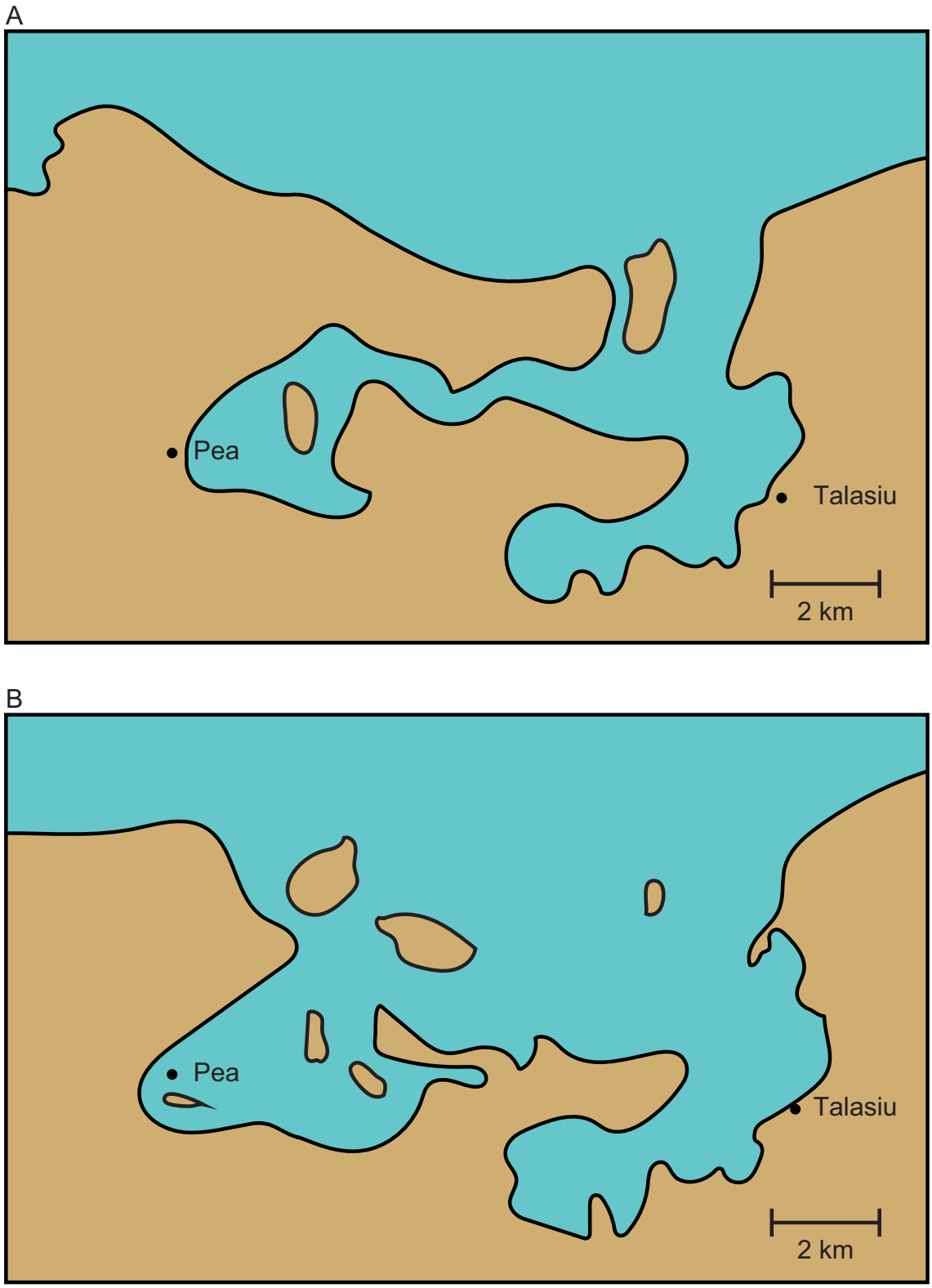

Figure 1-3. Modern (A) and mid-Holocene (B) schematic configurations of the north coast of Tongatapu at Fanga ‘Uta lagoon (modified from Dickinson 2007).

Chapter 2.

Development of novel proxy; lagoon-specific local marine reservoir effect –Application to Holocene sea level reconstruction with geophysical modeling in Tongatapu, Kingdom of Tonga–

Summary

Reconstructing the history of Holocene relative sea levels around Tonga provides essential constraints on the recent geological evolution of this region and paleoenvironmental context for archaeological studies. However, few sea level records are currently available in the region, and no quantitative paleoenvironmental studies using geochemical or geophysical methods have been reported. Here, we reconstruct Tongatapu Island's sea level history using radiocarbon measurements and glacio-hydro-isostatic adjustment (GIA) modeling. Our analyses reconstructing the lagoon's evolution suggest the average size of *Gafrarium tumidum* decreased synchronously with corresponding changes in the paleoenvironment. These changes also correspond to the increasing trend of the lagoon-specific local marine reservoir ages (ΔR_{lagoon}) from 105 ± 49 to 156 ± 85 years between ~2.6 and 1.2 ka. The minimum values of sea surface salinity (SSS) decline within Fanga'uta Lagoon was also synchronous with these changes caused by a gradual decrease in the exchange of water in and out of the lagoon. Freshwater input inferred from the shell was somewhat lower ca. 2.6 cal kyr BP than the present, suggesting the lagoon was relatively open to the ocean at that time. Our GIA modeling predicts mid-Holocene sea-level highstand (HHS) was less than 1 m above the present sea level in Tongatapu, suggesting previously reported observations of an HHS require additional contributions, perhaps from crustal uplift. Furthermore, recent Global Navigation Satellite System (GNSS) observations of vertical uplift rates at Tongatapu have a higher magnitude than the long-term uplift rate obtained from Holocene sea level data.

2.1. Introduction

2.1.1. Holocene sea level change and glacio-hydro isostasy

Sea level data during glacial-interglacial periods at sites far from former or current ice sheet regions (far-field) have been studied extensively using various proxies because they represent the mean state of past global climate (see Yokoyama *et al.,* 2019c). Temporal sea level changes since the Last Glacial Maximum (ca. 20 ka) thus provide information on ice sheet responses to global climatic changes (e.g., Kench *et al.,* 2020; Lambeck *et al.,* 2014; Yokoyama *et al.,* 2018) and environmental changes (e.g., Braga *et al.,* 2019; Humblet *et al.,* 2019; Webster *et al.,* 2018). Because the ice sheets in North America and northern Europe during the Last Glacial Maximum had entirely melted by ca. 7 ka, slow deformation induced by glacio-hydro-isostatic adjustment (GIA) of the Earth's surface was the dominant effect compared to polar ice volume changes during the mid-to-late Holocene (Clark *et al.,* 1978; Lambeck *et al.,* 2003). This deformation process modified past shoreline elevations: namely, the heights of relative sea level (RSL) indicators (Yokoyama & Esat, 2015).

The observed RSL is described as mathematically as follows (Lambeck et al., 2003):

$$\zeta_{RSL}(\phi, t) = \zeta_{gmsl}(\phi, t) + \zeta_{iso}(\phi, t) + \zeta_{tect}(\phi, t) - Eq.\,1$$

where $\zeta_{RSL}(\phi, t)$ describes the RSL changes at site φ between time t and the modern, $\zeta_{iso}(\phi, t)$ is the isostatic component of sea-level change which includes the effects of both ice and water loading, and $\zeta_{tect}(\phi, t)$ represents the tectonic component due to long term surface deformations other than GIA. Assuming the melt water from ice sheets s uniformly distributed over the oceans at time t, then $\zeta_{gmsl}(t)$ is given as:

$$\zeta_{gmsl}(\phi, t) = -\frac{\frac{\rho_i}{\rho_o \delta V_i(t)}}{A_o(t)} - Eq.\,2$$

where ρ_i and ρ_o represent the densities of ice and water respectively and $V_i(t)$ is the volume change of global, land-based ice. $A_o(t)$ is the surface area of the ocean at time t.

A Holocene sea level history for Tonga has been also reconstructed from uranium-series dating of corals (e.g., Bourrouilh & Hoang, 1976; Taylor, 1978) and pollen analysis of mangrove sediments (Ellison, 1989). The maximum sea level height during the mid-Holocene (ca. 6 ka, Figure 2-1) was at least 1.9 – 2.5 m higher than the modern sea level because of hydro-isostacy, but this attribution remains speculative; few quantitative modeling studies have explored the effects of GIA in Tonga.

Moreover, archaeological investigations on Tongatapu Island also suggest that sea levels declined about 2,500 years ago and that the closure of the bay led to a decrease in seawater salinity and increase of siltation. This resulted in a decrease in marine taxa (e.g., Clark *et al.,* 2015; Spennemann, 1987), but no quantitative paleoenvironmental studies using geochemical methods have been reported.

Figure 2-1. A mid-Holocene paleoshoreline notch at a beach near Anahulu cave (see Figure 3-1) on east coast of Tongatapu, the Kingdom of Tonga.

2.1.2. Quantification of rheological parameters and geophysical activities using GIA model

At many far-field sites, the RSL indicator of the mid-to late-Holocene is located above present-day sea level due to GIA and is called the Holocene High Stand (HHS). The magnitude and timing of the HHS depend mainly on local geophysical properties and whether tectonics derived from seismic activities. Therefore, in order to infer lithospheric thickness and mantle viscosities, former studies used systematic RSL observations together with GIA modeling (Mitrovica & Milne, 2002; Nakada & Lambeck, 1987; Yokoyama *et al.,* 2016).

The Kingdom of Tonga is composed of carbonate islands located at far-field sites in the South Pacific (Figure 1-1). The sites are also situated near the Tonga Trench, where large plate subduction-induced earthquakes have been reported (Lay *et al.,* 2010). Such massive earthquake-generated tsunamis have the potential to damage low-lying islands (e.g., Jackson *et al.,* 2014; Yokoyama *et al.,* 2019a). Thus, understanding the nature of tectonics in this region is crucial for coastal management efforts to mitigate tsunami hazards. The Fiji–Tonga region has complex tectonics as mentioned above. A GIA modeling approach can provide insight on the region's tectonics, comparing both short-term instrumental observations as well as long-term geological observations that can be useful to quantify geophysical activities near a plate boundary (e.g.,Yousefi *et al.,* 2020).

2.1.3. The aim of this chapter

In this study, the lagoon-specific marine reservoir effect (ΔR_{lagoon}; see methods section for definition), determined from archaeological shells, serves as a proxy of water exchange between the lagoon and the Pacific Ocean. Numerical GIA modeling is performed to explore relative sea level changes in Tongatapu. The results are compared with present-day satellite-based GNSS (GPS) observations of vertical land motions on the island to better understand the long-term tectonics in the region. I aim to evaluate the previously published proposal that the modification of the coastal landscape had been initiated at ca. 2.6 ka using geochemical and geophysical approaches.

2.2. Materials and Methods

2.2.1. Site Description and Sample Collection

Tongatapu Island (21° 08'S, 175° 12'W) is the largest island of the Kingdom of Tonga and is located ~200 km southeast of Fiji and ~2,000 km northeast of New Zealand (Figure 1-1). Tonga is in the subtropic zone, which is characterized by a warm, wet season from November to April and a cool, dry season from May to October. The rainfall is affected by the South Pacific Convergence Zone (SPCZ) in Tonga, and 60% of the annual rainfall comes during the wet season (Australian Bureau of Meteorology and Commonwealth Scientific and Industrial Research Organisation 2014).

The island has a freshwater lens that is recharged solely by rainfall, reaches a thickness of about 12 m at the center of Tongatapu, and discharges at the edges of the island (van der Velde *et al.,* 2006a). Because of the high permeability of the soil and underlying limestone in Tongatapu, surface water is scarce or nonexistent (White & Falkland, 2010), thus freshwater flow into Fanga 'Uta lagoon is almost from the freshwater lens. Despite high permeability, the evapotranspiration is so high that at most 20% to 30% of the rainfall reaches the freshwater lens (Hunt, 1979; van der Velde *et al.,* 2005; White *et al.,* 2009).

2.2.2. Sample collection and preparation

Sixty fossil samples of *Gafrarium tumidum*; Röding, 1798 were obtained from three archaeological sites in Talasiu and Lapaha on the eastern shore of Fanga'uta Lagoon (Figure 1-1). The ages of each site were determined based on the radiocarbon ages of charcoals. TO-Mu-2 was 2.6 cal kyr BP, J17 was 1.2 cal kyr BP, and J13 was 0.4 cal kyr BP (TO-Mu-2 and J17 Petchey & Clark, 2011; J13 Clark *et al*., in prep). Fourteen living *G. tumidum* specimens were collected from Nukunukumotu and Talasiu, but no live samples were found in Pea. In the laboratory, each shell's length and height were measured using a digital caliper to the nearest 0.01 mm (Figure 2-2).

We performed *in situ* measurements of sea surface temperature (SST) and sea surface salinity ($SSS_{in\ situ}$) in Nukunukumotu, Talasiu, and Pea (Figure 1-1). SST was measured monthly from December 2016 to November 2017 using a HOBO Water Temperature Pro v2 (± 0.2°C accuracy), and $SSS_{in\ situ}$ was measured in July and December 2016 and December 2017 using a portable salinometer (± 1 psu accuracy).

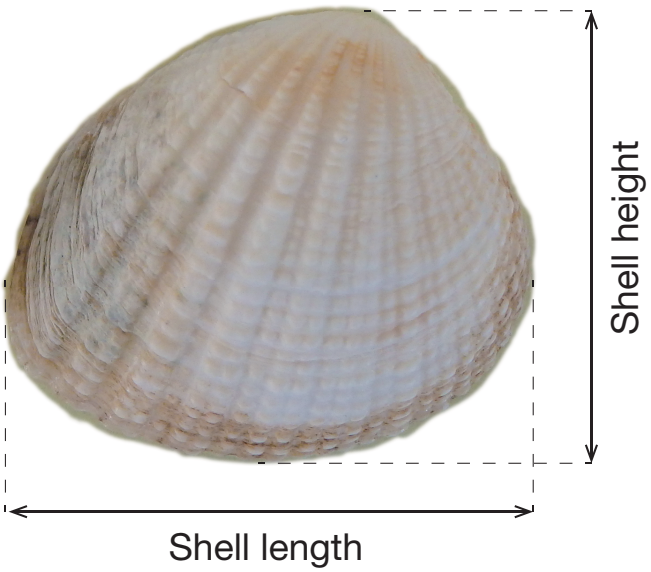

Figure 2-2 Shell measurements of *G. tumidum*, measured using digital calipers accurate to two decimal places.

2.2.3. Stable oxygen isotope analyses

本節については、5 年以内に雑誌等で刊行予定のため、非公開。

2.2.4. Radiocarbon dating

4 live and 30 fossils of *G. tumidum* specimens were used. I obtained approximately 10 mg of shell samples for radiocarbon dating by cutting the outer layer of the shell. After the physical cleaning of the shells, surface contamination was removed by etching with 1% HCl, and the shells were rinsed with Milli-Q water. The samples were then dissolved in 85% phosphoric acid in a vacuum tube. The CO_2 produced by dissolution was then passed through an ethanol-liquid nitrogen trap (at approximately −100°C) to purify the gas. The CO_2 was graphitized with 4–5 mg of Fe powder in a hydrogen atmosphere heated to ~630°C (see Yokoyama *et al.,* 2007; 2010). The resulting graphite was then placed into aluminum cathodes and analyzed at Atmosphere Ocean Research Institute, University of Tokyo, using a single-stage accelerator mass spectrometer following analytical protocol (Yokoyama *et al.,* 2019b).

2.2.5. Calculation of lagoon-specific marine reservoir effect (ΔR_{lagoon})

The marine reservoir age (R) is the difference between oceanic and atmospheric radiocarbon ages (Alves *et al.,* 2019; Hirabayashi *et al.,* 2019; Stuiver & Polach, 1977). Present-day global average values are approximately 400 years, but local marine reservoir age offsets (ΔR) are induced by local environmental conditions (Hirabayashi *et al.,* 2017; 2019). ΔR values are used as a proxy for local environmental conditions, including sea level changes (e.g., Lindauer *et al.,* 2017a).

In this chapter, I define the equation ΔR_{lagoon} as the difference between the ^{14}C activity of the open ocean and the lagoon-specific value at the same time to estimate the change in the lagoon's freshwater proportion.

$$\Delta R_{lagoon} = {}^{14}C\ age_{shell} - {}^{14}C\ age_{modeled\ global\ ocean}$$

As mentioned above, freshwater into Fanga ‘Uta lagoon is flowed through a freshwater lens. Freshwater would contain lower ^{14}C than seawater due to limestone solution in the freshwater lens. Therefore, ^{14}C content of lagoon water will indicate the ratio between ^{14}C content of freshwater and that of seawater, and bivalves living in the lagoon will also indicate the ratio.

A monospecific brackish bivalve (*G. tumidum*) throughout the time of interest were used in this study. *G. tumidum* is a suspension-feeding shellfish, and the ^{14}C values of its shell should reflect the ^{14}C values of dissolved inorganic carbon (DIC) from surface water (e.g., Lindauer *et al.,* 2017b; Nishida *et al.,* 2020; Petchey *et al.,* 2013; Petchey & Clark 2011). Thus, changes in radiocarbon in the ambient environments can be compared directly without any concerns related to vital effects. I recalculated ΔR using an online application (Reimer & Reimer, 2017) and the latest calibration data sets: ShCal20 (Hogg *et al.,* 2020) and Marine20 (Heaton *et al.,* 2020).

2.2.6. GIA modeling and shoreline reconstructions

I modeled GIA using Australian National University's CALSEA software (Lambeck *et al.* 2017) with nine iterations of the sea level equation (Lambeck *et al.,* 2003), a three-arc-minute global topography data set, and ice sheets using previous regional inversions (e.g., Lambeck *et al.,* 2010; 2017). Global mean sea level values for the combined ice sheets were tuned to match the time-series data of (Lambeck *et al.,* 2014; 2017). Calculations were performed for 560 distinct rheologies (Table 2-1) spanning the permissible parameter ranges for far-field ocean margin sites (Lambeck *et al.,* 2014). The range of predicted RSLs obtained from the 560 rheological models is shown in the figure as gray shading. Furthermore, I set six preferred rheological parameters appropriate for small oceanic islands far from continental margins (Lambeck 2002; Mitrovica & Milne 2002). Ice sheets (Woodroffe *et al.,* 2012) for the Tongatapu are listed in Table 2-2 and are depicted with symbols on predicted sea level curves in Figure 2-3.

I mapped shoreline around Fanga'uta Lagoon indicating where the area is key to separate between inside and outside the lagoon (Figure 2-4). This high-resolution map was produced based on aerial topographic and bathymetric lidar data acquired by the Tongan government as a component of the AusAID-funded (presently Australian Aid) Pacific Adaption Strategies Assistance Program over Tongatapu. Topographic lidar measurements were acquired during six flights between October 3 and October 24, 2011, and bathymetric lidar measurements were acquired during eight flights between September 5 and September 15, 2011. Lidar data were captured on the WGS84 horizontal datum and projected onto the Tonga Map Grid 2005. The vertical datum used in the survey was the Earth Gravitational Model 2008 geoid, and the contractor made a local adjustment of 0.77 m to adjust the vertical datum to mean sea level at the benchmark

TON1 vide the Nuku'alofa Sea Level Fine Resolution Acoustic Measuring Equipment tide gauge. The vertical accuracy of the topographic lidar data is ± 0.15 m (1 SD), and that of the bathymetric lidar data is ± 0.50 m (1 SD). GIA modeling results were analyzed alongside the topographic and bathymetric lidar to infer paleolandscape changes.

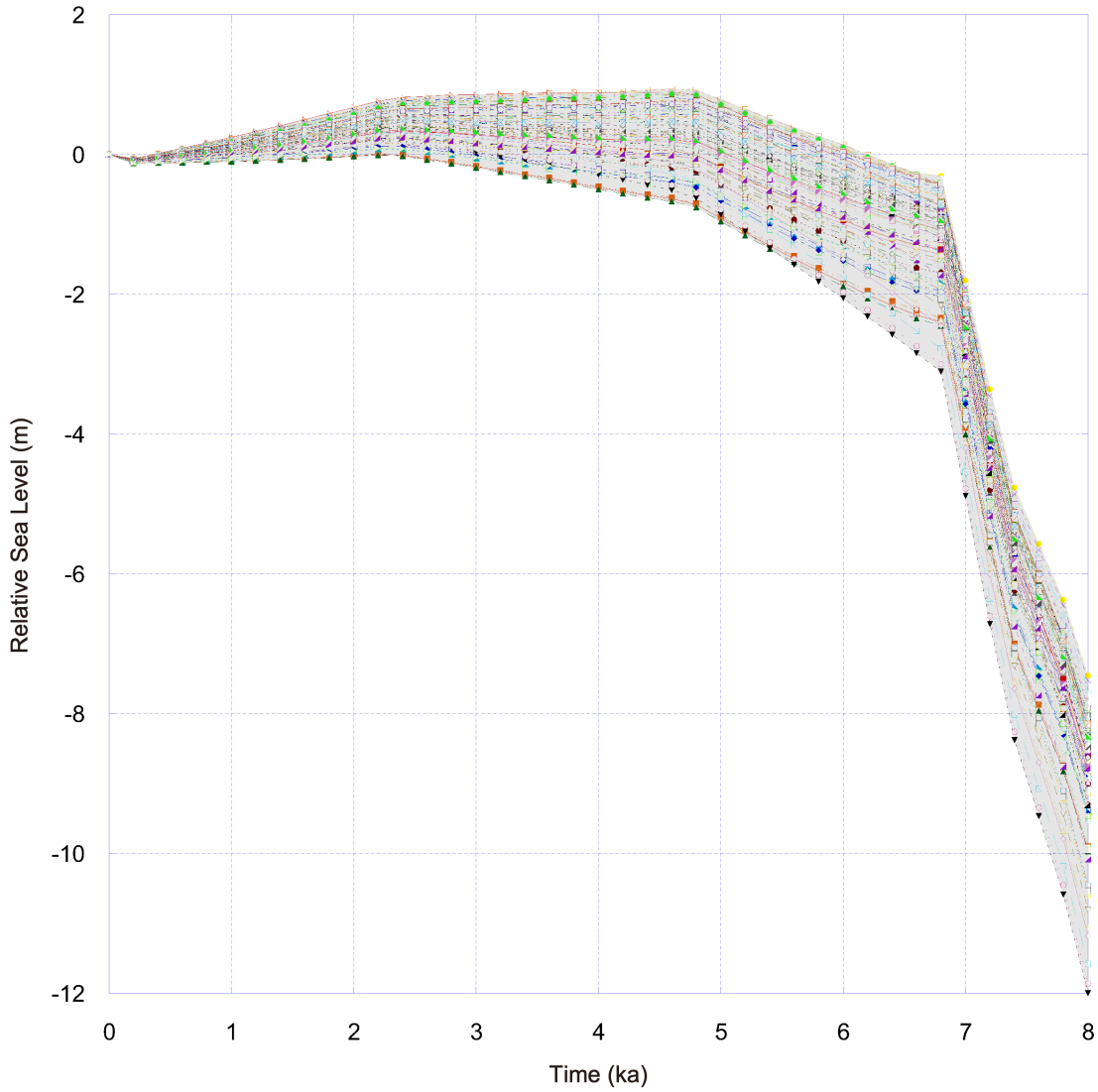

Figure 2-3. RSL changes predicted by the GIA model used all rheological parameters around Tongatapu Island. Modified from (Fukuyo *et al.,* 2020).

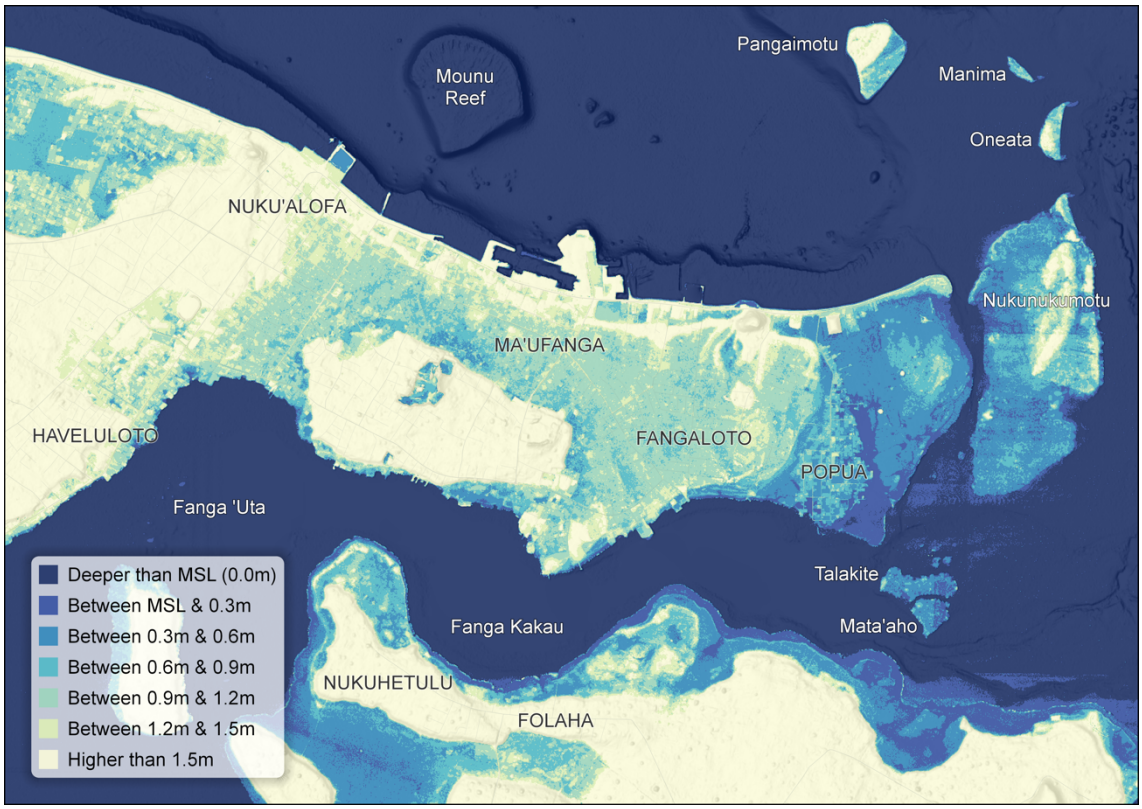

Figure 2-4. High-resolution topographic map based on lidar data around Fanga'uta Lagoon in Tongatapu (Fukuyo *et al.,* 2020).

Table 2-1. Rheological parameters used for 560 GIA model runs.

Lithospheric thickness (km)	60, 65, 70, 80, 90, 100, 110, 120
Upper mantle viscosity (10^{20} Pa s)	0.7, 1, 2, 3, 4, 5, 6, 10, 20, 30
Lower mantle viscosity (10^{21} Pa s)	3, 5, 7, 10, 30, 50, 100

Table 2-2. Representative rheological parameters for the Tongatapu used for GIA modeling.

Lithospheric thickness (km)	Upper mantle viscosity (10^{20} Pa s)	Lower mantle viscosity (10^{21} Pa s)
65	4	10
65	0.7	10
50	2	10
100	2	10
65	2	30

2.3. Results

2.3.1. Modern seawater temperature and salinity measurements

SSTs observed between December 2016 and November 2017 at Nukunukumotu, Talasiu, and Pea varied from 20.9 to 30.1°C, from 22.5 to 32.1°C, and from 20.3 to 31.9°C, respectively (Figure 2-5). A paired *t*-test among the three sites (Nukunukumotu-Pea, p = 0.39; Talasiu-Pea, p = 0.55; Nukunukumotu-Talasiu, p = 0.13; with $p < 0.05$ indicating statistically significant differences) indicates there is no spatial variation in the lagoon's SST.

In contrast to SST, $SSS_{in\ situ}$ varied noticeably among the three sites. $SSSs_{in\ situ}$ observed between December 2016 and December 2017 at Nukunukumotu, Talasiu, and Pea ranged from 27.0 to 31.5, from 16.0 to 26.0, and from 11.0 to 13.5 psu, respectively (Table 2-3). Due to increased precipitation in December (during Tonga's rainy season), $SSSs_{in\ situ}$ at all sites should be lower in December than in July. However, SSSs at Talasiu and Pea in austral summer were higher than in austral winter because of sudden rainfall during the July 2016 field survey.

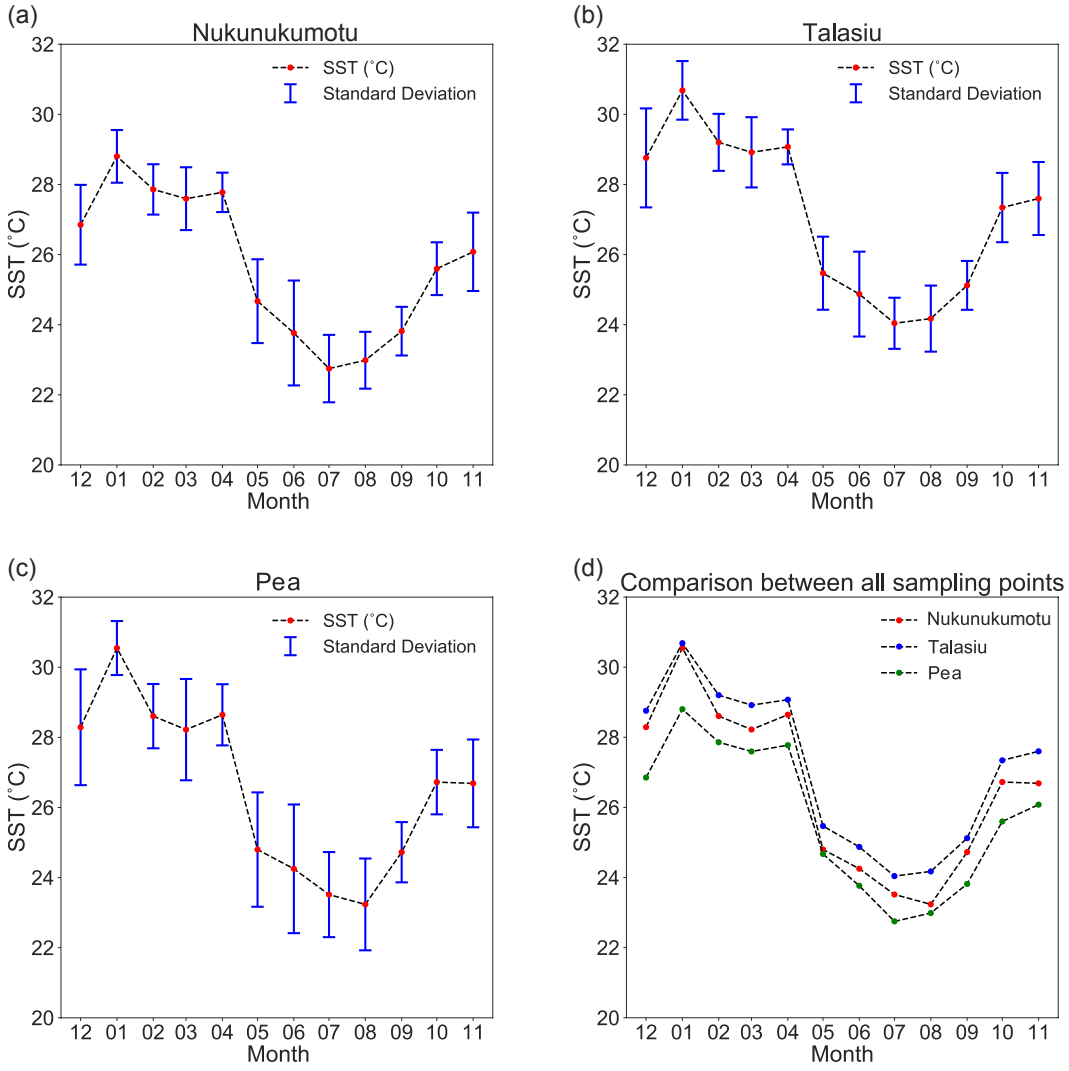

Figure 2-5. Monthly averaged SSTs from December 2016 to November 2017 at (a) Nukunukumotu, (b) Talasiu, and (c) Pea (error bars are 1 SD). (d) Comparison among all sampling sites (Fukuyo *et al.,* 2020).

Table 2-3. Sea surface salinities ($SSSs_{in\ situ}$) in summer and winter at each site.

Site name	SSS in summer* (December 2016)	SSS in winter (July 2016)
Nukunukumotu	27.0 ± 1.0	31.5 ± 1.0
Talasiu	26.0 ± 1.0	16.0 ± 1.0
Pea	13.5 ± 1.0	11.0 ± 1.0

2.3.2. $\delta^{18}O$ composition of seawater

本節については、5 年以内に雑誌等で刊行予定のため、非公開。

2.3.3. Shell size of *G. tumidum*

本節については、5 年以内に雑誌等で刊行予定のため、非公開。

2.3.4. $\delta^{18}O$ composition of shells

本節については、5 年以内に雑誌等で刊行予定のため、非公開。

2.3.5. Radiocarbon measurements and ΔR_{lagoon}

本節については、5 年以内に雑誌等で刊行予定のため、非公開。

2.3.6. GIA modeling

I used CALSEA software to model RSL around Tongatapu Island during the past 6,000 years. The results omit a 20 cm meltwater pulse since 1850 from Antarctica, Greenland, and mountain glaciers, which reflects recent sea level rise (Lambeck *et al.,* 2017). Except for the extreme case of a high upper mantle viscosity (red curve, Figure 2-10), the models indicate the Holocene highstand (HHS) occurred around 2.5 ka and was driven by eustatic sea level rise. Modeled HHSs ranged from 0.2 to 0.4 m in elevation, but no model—except for cases when extreme rheological parameters were employed—suggested a higher HHS elevation in Tongatapu. All sea level models show a monotonic decrease in RSL after the HHS at ca. 2.5 ka using this ice model (i.e., ANU model; Lambeck *et al.,* 2014) because the cessation of global ice volume decrease was marked at this time (Figure 2-3 and 2-10).

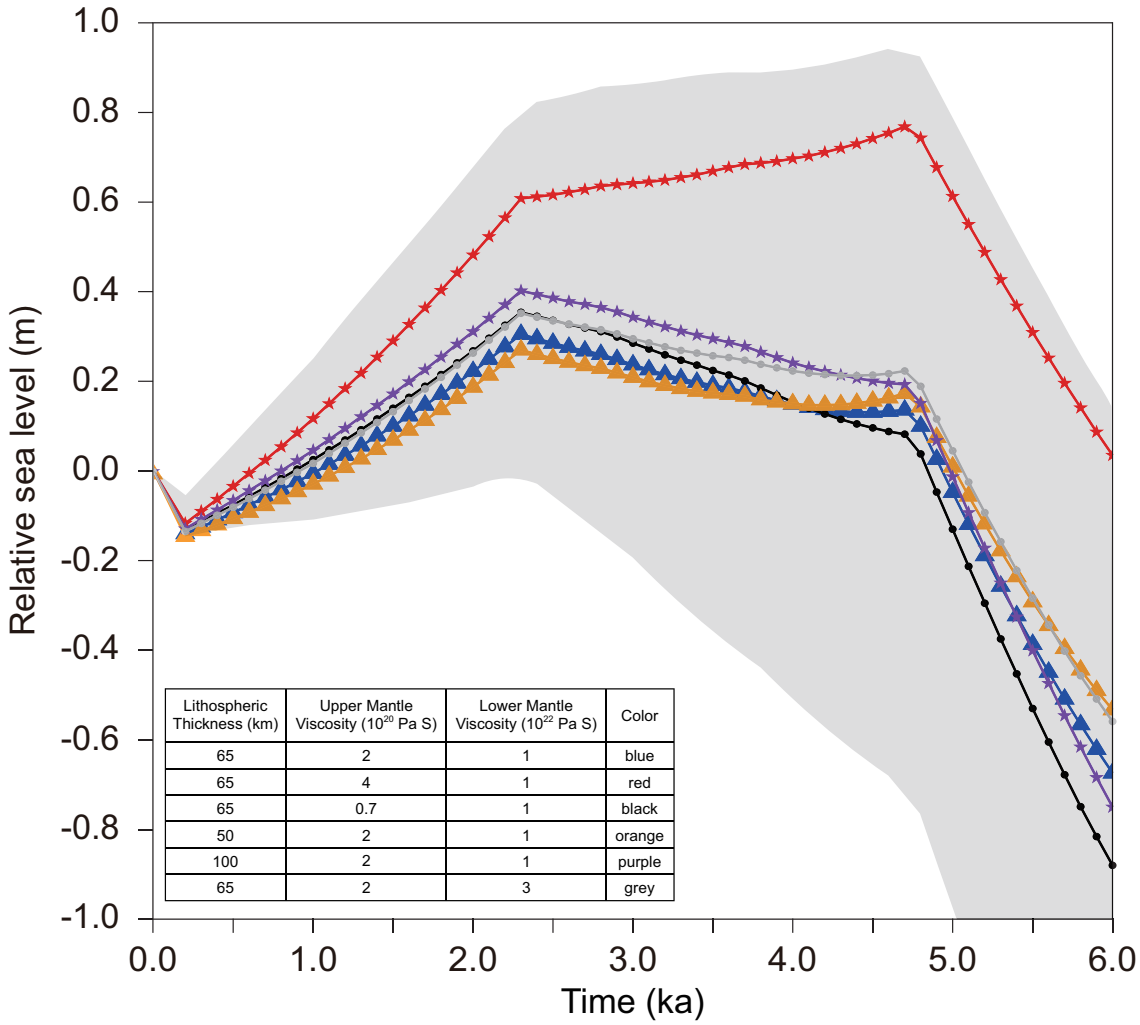

Figure 2-10. RSL changes predicted by the GIA model around Tongatapu Island. The gray shading is the range of predicted RSLs obtained from 560 rheological models.

2.4. Discussion

2.4.1. The Relationship between $SSS_{in\ situ}$ and $\delta^{18}O_{sw}$ in Fanga' Uta lagoon

本節については、５年以内に雑誌等で刊行予定のため、非公開。

2.4.2. Relationship between $\delta^{18}O_{shell}$ and SST and $SSS_{in\ situ}$ in Fanga' Uta lagoon

本節については、5 年以内に雑誌等で刊行予定のため、非公開。

2.4.3. Reconstruction of SSSs using fossil bivalves in Fanga' Uta lagoon and its limitation

本節については、5 年以内に雑誌等で刊行予定のため、非公開。

2.4.4. Suitability of *G. tumidum* ^{14}C as a proxy for ΔR_{lagoon}

本節については、5 年以内に雑誌等で刊行予定のため、非公開。

2.4.5. Holocene changes in lagoon water properties inferred from the ΔR_{lagoon} of *G. tumidum*

本節については、5 年以内に雑誌等で刊行予定のため、非公開。

2.4.6. Paleotopographic reconstruction

I reconstructed the topography map of Tongatapu by subtracting gridded RSL values from modern bathymetry and topography maps (Figure 2-4). The colors show the areas where different relative sea levels potentially make the opening of the lagoon mouth at the Fanga'uta Lagoon in Tongatapu. According to the shell ΔR_{lagoon} and size changes described in the above section, sea level has been falling since 2.6 ka. Hence, a minimum 1.0 m to 1.5 m higher relative sea level in Tongatapu should had occurred at 2.6 ka.

To examine whether GIA-induced relative sea level changes during this time could produce this magnitude, we have conducted GIA modeling using various Earth viscosity models (Figure 2-3). The results suggest RSL at ca. 2.5 ka was likely only approximately 20–80 cm higher than today, lower than that required to make an opening of the lagoon mouth. Thus, an additional factor to produce at least ~50 to 100 cm of crustal vertical uplift/relative sea level fall is required.

2.4.7. Comparison of GIA modeling to sea level indicators and GNSS (GPS) observation

The highest mid-Holocene HHS estimated from our GIA-preferred model results was ~0.75 m around 5 ka for an Earth model consisting of a 65 km-thick elastic lithosphere with upper and lower mantle viscosities of 4×10^{20} and 1×10^{22} Pa s, respectively (Figure 2-10). For comparison, earlier studies using fossil corals as sea level indicators have reported sea level increases of 1.9 to 2.2 m in Tongatapu around 6 ka (Figure 2-18; Bourrouilh & Hoang, 1976; Taylor, 1978; Woodroffe, 1983). Many previous studies suggest RSL changes in Tongatapu were driven primarily by hydro-isostasy (e.g., Dickinson *et al.,* 1999; Spennemann, 1997); however, without conducting actual GIA modeling, I confirmed a GIA-induced HHS of 0.5 – 0.8 m.

This suggests GIA may not be solely, nor even primarily, responsible for the observed vertical land motion at this location. Near a subduction zone, interseismic deformation can be observed or modeled. A comparable example may be seen in the site similarly close to the subduction zone in Japan. After the 1946 earthquake in the Nankai area, approximately 10 mm/year uplifts were observed as early stage interseismic deformation at a site located about 200 km from the Nankai subduction zone (Li *et al.,* 2020; Wang & Tréhu, 2016). Tongatapu Island is also located approximately 200 km from the Tonga Trench. The most recent large earthquake (M_w 8.1) occurred along the Tonga Trench in 2009 (Fritz *et al.,* 2011). The GNSS records for Tongatapu during the past 10 years (http://www.sonel.org) show an average uplift velocity of 3.01 ± 0.41 mm/year. This can be attributed to the early stage of interseismic vertical deformation in Tongatapu. If this velocity is extrapolated for the past 6,000 years, then sea level indicators formed ca. 6 ka are expected to be located at about 18 m higher than the present-day sea level (Figure 2-18). This number is much higher than the sea level indicator of the island using fossil

coral samples. Thus, it suggests the recent observed uplift velocity of Tongatapu Island with GNSS is a relatively short and recent phenomenon and not the one that has been continuing during the past 5,000 years.

The results of our GIA modeling further suggest RSL decreased sharply after 2.25 ka. This timing is coeval with the age of change in the Tongatapu Island marine ecosystem recorded by Clark *et al.* (2015).

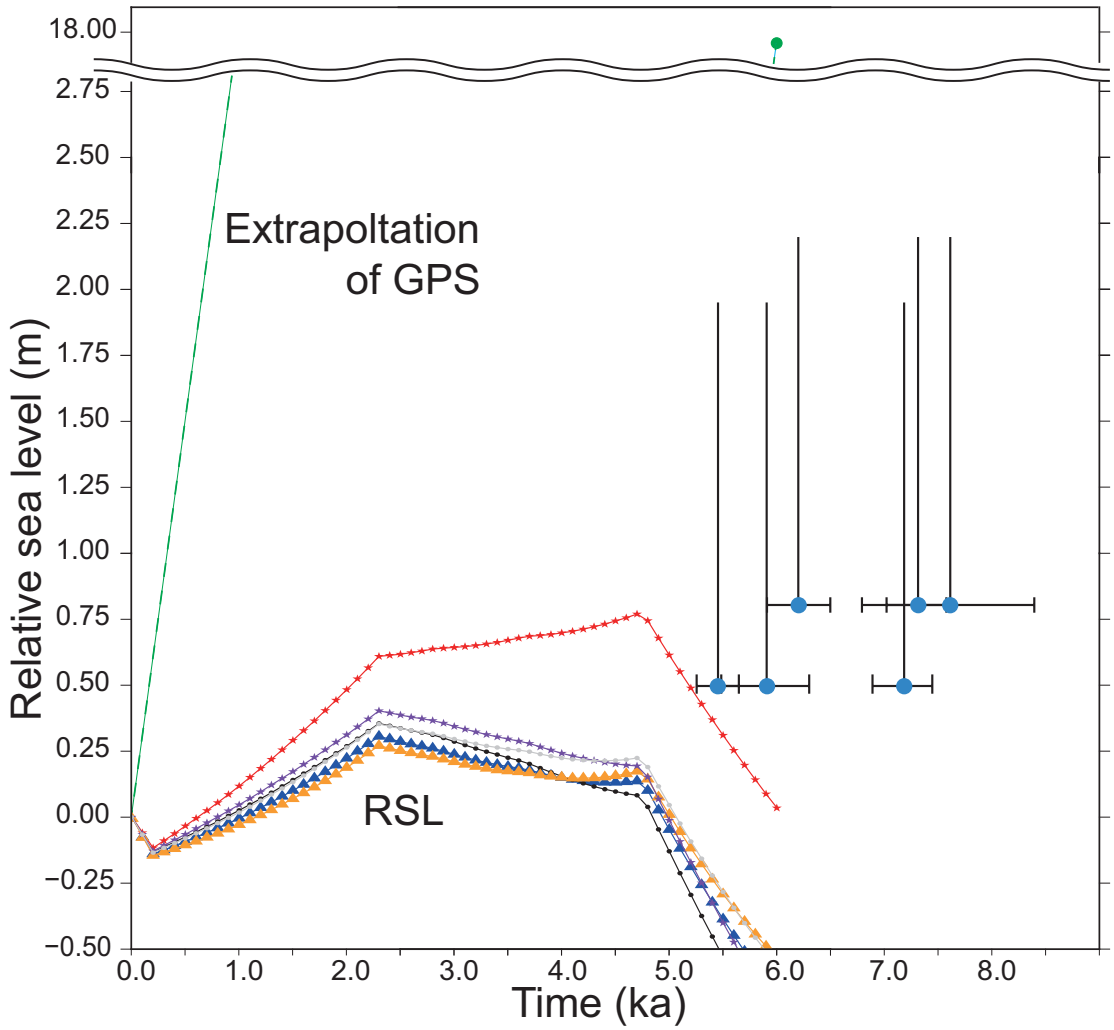

Figure 2-18. Comparison among RSLs obtained from our GIA model (lines as in Figure 2-10), sea level indicators (evidence of Holocene highstand) obtained from fossil corals (blue points; Bourrouilh & Hoang, 1976; Taylor, 1978; Woodroffe, 1983, vertical lines; tidal ranges), and extrapolation from recent GNSS observations (green dashed line and point, note break in scale). I recalculated the calendar ages of corals using OxCal v4.3 (Ramsey, 2009b) and the Marine13 calibration curve (Reimer *et al.,* 2013). ΔR is 87 ± 74 ^{14}C years (Petchey & Clark, 2011). From Fukuyo *et al.* (2020).

2.4.8. Comparison of previously reported sea level indicators with GIA predictions and ΔR_{lagoon}

I compared RSLs obtained from our GIA model, sea level indicators (Bourrouilh & Hoang, 1976; Taylor, 1978; Woodroffe, 1983), and sea level records estimated by combining RSLs and the lidar data set (Figure 2-19). According to archaeological studies (e.g., Clark *et al.,* 2015), the near closure of the lagoon started ca. 2.5 ka. Moreover, based on our paleotopographic mapping, a sea level drop of ~50 to 100 cm is required to have closed the lagoon. Considering the tidal range at Tongatapu, the near closure of the lagoon ca. 2.5 ka can be explained by a sea level drop due to ocean syphoning (e.g., Johnston 1993; Mitrovica & Milne 2002) consistent with the RSLs obtained in our GIA model. In addition, the sea level fell steadily after this period, which led to the lagoon's monotonic closure. Thus, the freshwater input into the lagoon has increased steadily due to reduced exchange between the lagoon and the open sea, consistent with the continuous increase of ΔR_{lagoon} values over the past 2,500 years (Clark *et al.,* 2015). By contrast, fossil corals indicate ca. 6 ka the sea level was up to 1 m higher than the maximum sea levels ca 2.5 ka as estimated by the GIA model, suggesting not only ocean syphoning but also crustal uplift contributed to the observed sea level change at Tongatapu.

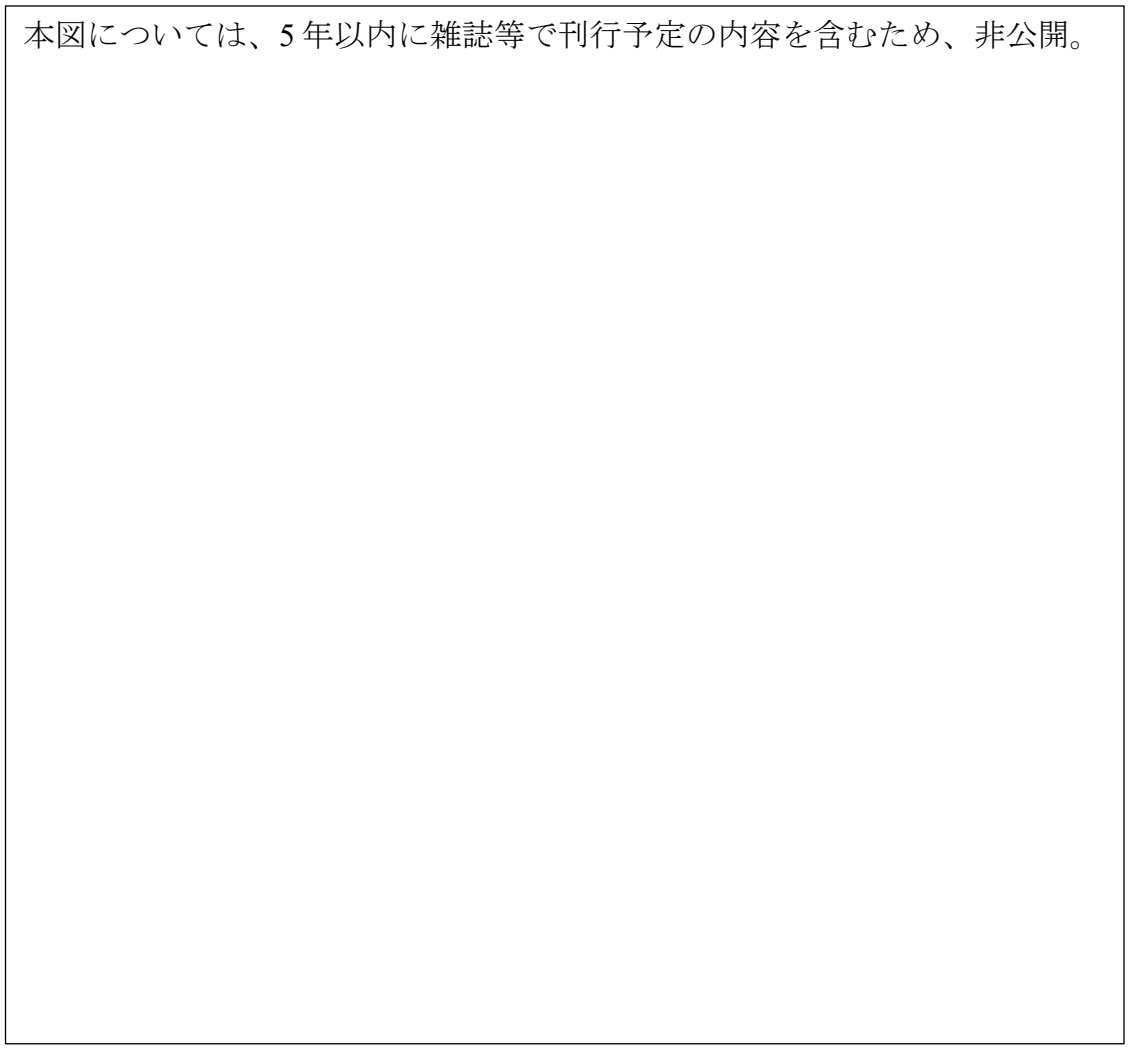

Figure 2-19. Comparison of RSLs obtained from fossil corals (blue symbols, vertical lines: tidal ranges), our GIA model (lines as in Figure 2-10), and ΔR_{lagoon} (t) values indicating a trend of decreasing salinity since ca. 2.5 ka. The green point indicates a sea level drop required to close the lagoon according to our topographic mapping.

2.4.9. Shell sizes related to paleoenvironmental changes

As discussed earlier, I employed only the monospecific bivalve *G. tumidum* to reconstruct the environmental change of the lagoon during the Holocene period. Thus, no interspecific variations are needed to be considered to infer causation of changes observed in this study.

Further, it is suitable to discuss the change in shell size because the *G. tumidum* collected in this study should not be juvenile. They obtain the first sexual maturity about 20 mm in shell height on the coasts of southeast India (Jagadis & Rajagopal, 2007) and southwestern New Caledonia (Baron 1992). The lengths of all shells used in this study were at least 20 mm (Tables 2-6 and 2-8, Figure 2-6). In addition, oxygen isotope analysis in this study suggests that some samples have 2–3 year cyclicities in their outer layers.

Alternatively, human predation can influence shell size because larger individuals of a species are targeted preferentially (Mannino & Thomas, 2002). Currently, it is impossible to completely disentangle the effects of SSS and human predation on shell size, although Clark *et al.* (2015) did not record a decrease in shell size at the Talasiu site, where *G. tumidum* has been harvested intensively.

As GIA model, paleotopographic reconstruction, and ΔR_{lagoon} of *G. tumidum* showed the lagoon was increasingly enclosed at ~2.5 ka involving environmental changes, including an increase in freshwater inflow and grain refining of bottom sediment. In the archeological site of Talasiu at 2.6 ka, *A. antiquata* and corals, which prefers sandy substrates and saline conditions, were found, but they inhabit in only lagoon mouth, whereas *G. tumidum,* which prefer more muddy blackish condition is abundant in modern Talasiu (Zann, 1984). Moreover, the shell sizes of present-day *G. tumidum* seem to be controlled more by SSS than by SST (Table 2-13), as demonstrated by the absence of *G.*

tumidum in the innermost part of the lagoon (Pea), where the salinity is dramatically lower. This result is consistent with the incipient lower salinity limit of < 16 psu for *G. pectinatum* (Mcmahon, 2003). Hence, the alteration of salinity and sediments in the lagoon due to sea level change can affect the ecosystem in the lagoon, including the shift of marine taxa and the size change of organisms.

Table 2-13. Shell sizes of living *G. tumidum* and physical seawater properties.

Area	Average shell height (mm)	Average SSS	Average SST (°C)
Nukunukumotu	24.7 (n = 7)	29.3	25.7
Talasiu	29.8 (n = 7)	21.0	27.1
Pea	-	12.3	26.5

2.5. Conclusion

I have investigated relative sea level changes at Tongatapu using ΔR_{lagoon} values and shell sizes of *G. tumidum*, paleotopographic mapping, and GIA modeling. Our main conclusions are summarized as follows.

1) ΔR_{lagoon} values of prehistoric bivalves show an increased influx of old ^{14}C from terrestrial limestone to Fanga'uta Lagoon between ~2.6 cal kyr BP and present day. I tentatively attribute this to the near closure of the lagoon, consistent with the scenario Clark *et al.* (2015) presented.

2) GIA modeling suggests the contribution of ocean syphoning to sea level changes at Tongatapu was smaller than previously estimated.

3) Paleotopographic maps reconstructed from topographic data and GIA modeling indicate the near closure of the lagoon ca. 2.5 ka, consistent with our ΔR_{lagoon} results and those of Clark *et al.* (2015). This suggests ΔR serves as a reliable geochemical proxy of small-scale environmental changes, which can be reconstructed when combined with high-resolution topographic data.

4) SSS decrease and siltation increase due to the closure of the lagoon would have had significant negative impacts on the lagoon environment such as the decline in bivalve body size over the past 2,600 years.

5) Recent GNSS observations of vertical land motion at Tongatapu are inconsistent with paleoshoreline data, suggesting the recent uplift trend is not characteristic of the past 2,600–6,000 years.

Chapter 3. High spatial resolution magnetic mapping using ultra-high sensitivity scanning SQUID microscopy on a speleothem from the Kingdom of Tonga, southern Pacific

本章については、5 年以内に雑誌等で刊行予定のため、非公開。

Chapter 4. General conclusion and Future work

4.1. General conclusion

本節については、5 年以内に雑誌等で刊行予定の内容を含むため、非公開。

4.2. Future perspectives

4.2.1. Linking environmental changes to human activities in the South Pacific

In the Pacific, a number of archaeological sites have a similar geological setting (e.g., Dickinson 2014; Kayanne *et al.,* 2011; Petchey *et al.,* 2018). The end of early settlement in the western Pacific island groups (e.g., Fiji, Papua New Guinea, Mariana, New Caledonia, and Vanuatu) clusters tightly around 2500 cal yr B.P. (e.g., Carson & Kurashina 2012; Denham *et al.* 2012; Irwin *et al.* 2011). The synchronicity of this event over this extremely wide region can suggest that it was externally driven. Previous studies suggest that the 0.7 m on average sea-level fall occurred within the western Pacific Ocean from 3500 to 2000 cal yr B.P. (e.g., Nunn and Carson, 2015). Therefore, sea-level change in that era seem to be the key drivers that could have uniformly and synchronously impacted the coastal environment and residents in these island groups in this region. However, few studies have been published on the relationship sea level fall and paleoenvironmental changes using geochemical methods in this region.

I showed that ΔR_{lagoon} could be a novel proxy for the ratio of inflow content of ^{14}C in freshwater through terrestrial limestone and the relationship between RSL change in the Holocene and its driving paleoenvironmental changes (see in Chapter 2). The result in Chapter 2 can provide an example of the end of early settlement in the western Pacific island groups based on geochemical evidence.

Moreover, Nunn (2000) suggests that temperature fall and sea-level fall — characterized as the "A.D. 1300 event" — brought environmental and cultural changes on Pacific islands between the Medieval Warm Period and Little Ice Age. The event has been reported in several Pacific islands (e.g., Fiji (Kumar *et al.,* 2006); Easter island (Rull *et al.,* 2015); and Palau (Clark & Reepmeyer, 2012), and the environmental and cultural

effects driven by the event were complex. Thus, isolating each effect will require reconstructing past climate-environment-culture systems in the Pacific islands with geographically focused high-resolution data.

G. tumidum used in this study is food-species and widely preserved in archaeological sites in the Pacific. Therefore, there is a possibility that the shell can provide in other regions to reconstruct local paleoenvironmental changes such as sea-level changes that can be directly linked both spatially and temporally to records of human activities.

4.2.2. Estimations of vertical land motion over different time scales

In Chapter 2, I suggested that GIA may not be solely, nor even primarily, responsible for the observed RSL in Tonga. Tonga is located on the crest of the Tonga ridge parallel to the Tonga trench, where the rates of subduction are fast (24 – 6 cm/year: Smith and Price, 2006) and the geometry of the subducted Pacific slab beneath Tonga is complicated (see in Chapter 1). Especially, it is essential to understand the mantle structure of Earth with separation of the components with each different time-scale and this study investigated the combination between the GIA model, GNSS, and geomorphological evidence in Tonga. Thus, isolating the signal-associated GIA process and other tectonic the vertical signal associated with the regional and local tectonics.

For example, Yousefi et al. (2020) determined late Holocene (past 4000 years) VLM rates using RSL observations from the west coast of North America by isolating the GIA signal and compared these to decadal rates estimated from GPS. The VLM rates in the late Holocene corrected for the GIA contribution to RSL change indicated that data all areas except for the northwestern Strait of Georgia and central-western Vancouver Island. Conversely, The GPS-inferred VLM rates indicated uplifts at many sites compared to the

RSL-estimated rate. The GPS-inferred VLM rates were interpreted as being dominated by interseismic deformation, which occurred by postseismic viscoelastic relaxation after the earthquake and decays through time, associated with the locking of the Cascadia megathrust.

As mentioned above, the RSL during the mid-Holocene in Tonga is reported as ca. 1.9 to 2.2 m (see in Section 2.1.1), and the GIA contribution to RSL change is 0.5 – 0.8 m (see in 2.4.5); thus, the VLM rate over the past 6 ka corrected for the GIA contribution to RSL change can be inferred ca. 0.2 – 0.25 mm/year. Conversely, Tonga's GPS data show ca. 3 mm/year uplift, and it is much greater than the VLM rate. Moreover, in 2006 and 2009, large earthquakes occurred in Tonga (8.0 and 7.6 Mw, respectively), and the GPS recorded experience sudden subsidence of more than 10 mm. Therefore, the GPS-inferred VLM in Tonga also reflects interseismic deformation the same as Cascadia, and it suggests that the fault is locked and strain accumulates toward the next megathrust earthquake. In the future, I can estimate the current locking state of the Tonga trench by using a viscoelastic finite element model, which is developed by Li *et al.,* (2018) to invert from the horizontal components of the GPS data.

4.2.3. The potential of speleothem as environmental proxies

本節については、5 年以内に雑誌等で刊行予定のため、非公開。

Reference

Abe, O., S. Agata, M. Morimoto, M. Abe, K. Yoshimura, T. Hiyama & N. Yoshida, 2009. A 6.5-year continuous record of sea surface salinity and seawater isotopic composition at Harbour of Ishigaki Island, southwest Japan, *Isotopes in environmental and health studies* 45(3), 247–58.

Abrajevitch, A. & K. Kodama, 2011. Diagenetic sensitivity of paleoenvironmental proxies: A rock magnetic study of Australian continental margin sediments: DIAGENESIS, *Geochemistry, Geophysics, Geosystems* 12(5), .

Alves, E.Q., K. Macario, P. Ascough & C. Bronk Ramsey, 2018. The Worldwide Marine Radiocarbon Reservoir Effect: Definitions, Mechanisms, and Prospects, *Reviews of geophysics* 56(1), 278–305.

Alves, E.Q., K.D. Macario, F.P. Urrutia, R.P. Cardoso & C. Bronk Ramsey, 2019. Accounting for the marine reservoir effect in radiocarbon calibration, *Quaternary science reviews* 209, 129–38.

Australian Bureau of Meteorology and Commonwealth Scientific and Industrial Research Organisation, 2014.

Baldini, J.U.L., F. McDermott, A. Baker, L.M. Baldini, D.P. Mattey & L.B. Railsback, 2005. Biomass effects on stalagmite growth and isotope ratios: A 20th century analogue from Wiltshire, England, *Earth and planetary science letters* 240(2), 486–94.

Baron, J., 1992. Reproductive cycles of the bivalva molluscs Atactodea striata (Gmelin), Gafarium tumidum Roding and Anadara scapha (L.) in New Caledonia, *Marine and Freshwater Research* 43(2), 393–401.

Becker, S.O., I. Grosfeld, P. Grosjean, N. Voigtländer & E. Zhuravskaya, 2020. Forced Migration and Human Capital: Evidence from Post-WWII Population Transfers, *The American economic review* 110(5), 1430–63.

Bohnenstiehl, D.R., R.P. Dziak, H. Matsumoto & T.-K.A. Lau, 2013. Underwater acoustic records from the March 2009 eruption of Hunga Ha'apai-Hunga Tonga volcano in the Kingdom of Tonga, *Journal of Volcanology and Geothermal Research* 249, 12–24.

Bourrouilh, F. & C. Hoang, 1976. Uranium-thorium age of some corals from Tongatapu, in *Proceedings of International Symposium on Geodynamics in the South West Pacific, Noumea, New Caledonia*, 1–10.

Braga, J.C., Á. Puga-Bernabéu, K. Heindel, M.A. Patterson, D. Birgel, J. Peckmann, I.M. Sánchez-Almazo, J.M. Webster, Y. Yokoyama & R. Riding, 2019.

Brown, J.R., M. Lengaigne, B.R. Lintner, M.J. Widlansky, K. van der Wiel, C. Dutheil, B.K. Linsley, A.J. Matthews & J. Renwick, 2020. South Pacific Convergence Zone dynamics, variability and impacts in a changing climate, *Nature Reviews Earth & Environment* 1(10), 530–43.

Bryan, E., K.T. Meredith, A. Baker, M.S. Andersen, V.E.A. Post & P.C. Treble, 2020. How water isotopes (18O, 2H, 3H) within an island freshwater lens respond to changes in rainfall, *Water research* 170, 115301.

Burley, D., K. Edinborough, M. Weisler & J.-X. Zhao, 2015. Bayesian modeling and chronological precision for Polynesian settlement of Tonga, *PloS one* 10(3), e0120795.

Burley, D.V., W.R. Dickinson, A. Barton & R. Shutler, 2001. Lapita on the Periphery. New data on old problems in the Kingdom of Tonga, *Archaeology in Oceania* 36(2), 89–104.

Carson, M.T. & H. Kurashina, 2012. Re-envisioning long-distance Oceanic migration: early dates in the Mariana Islands, *World archaeology* 44(3), 409–35.

Cashman, K.V. & G. Giordano, 2008. Volcanoes and human history, *Journal of Volcanology and Geothermal Research* 176(3), 325–29.

Chand, S.S., 2020. Climate Change Scenarios and Projections for the Pacific, in *Climate Change and Impacts in the Pacific*, ed. L. Kumar. Cham: Springer International Publishing, 171–99.

Chen, Q., T.W. Zhang, Y.T. Wang, J.X. Zhao, Y.X. Feng, W. Liao, W. Wang & X.Q. Yang, 2019. Magnetism Signals in a Stalagmite From Southern China and Reconstruction of Paleorainfall During the Interglacial-Glacial Transition, *Geophysical research letters* 46(12), 6918–25.

Childs, C.W. & A.D. Wilson, 1983. Iron oxide minerals in soils of the Ha'apai group, Kingdom of Tonga, *Soil Research* 21(4), 489–503.

Clark, G., E. Grono, E. Ussher & C. Reepmeyer, 2015. Early settlement and subsistence on Tongatapu, Kingdom of Tonga: Insights from a 2700–2650calBP midden deposit, *Journal of Archaeological Science: Reports* 3(C), 513–24.

Clark, G. & C. Reepmeyer, 2012. Last millennium climate change in the occupation and abandonment of Palau's Rock Islands, *Archaeology in Oceania* 47(1), 29–38.

Clark, J.A., W.E. Farrell & W.R. Peltier, 1978. Global Changes in Postglacial Sea Level: A Numerical Calculation 1, *Quaternary Research* 9(3), 265–87.

Columbu, A., R. Drysdale, J. Hellstrom, J. Woodhead, H. Cheng, Q. Hua, J.-X. Zhao, P. Montagna, E. Pons-Branchu & R.L. Edwards, 2019. Investigation of the U-Th and radiocarbon dating of calcite speleothems from gypsum caves: Implication for palaeoclimate research, *Quaternary geochronology*.

Cook, J., 1777. A voyage towards the South Pole and around the world performed in His Majesty's ships the "Resolution" and "Adventure" in the years 1772--75, *London, Shanan and Cadell*.

Cowie, J.D., P.L. Searle, J.P. Widdowson & G.E. Orbell, 1991. Soils of Tongatapu, Kingdom of Tonga, *DSIR Land Resources, Lower Hutt*.

Cunningham, J.K. & K.J. Anscombe, 1985. *Geology of'Eua and Other Islands, Kingdom of Tonga*.

Damlamian, H., 2008. Tonga technical report, hydrodynamic model of Fanga'uta lagoon: water circulation and applications, *EUEDF-SOPAC: Reducing Vulnerbility of Pacific ACP States*. Project Report 135.

de Boer, C.B., T.A.T. Mullender & M.J. Dekkers, 2001. Low-temperature behaviour of haematite: susceptibility and magnetization increase on cycling through the Morin transition, *Geophysical Journal International* 146, 201–16.

Denham, T., C.B. Ramsey & J. Specht, 2012. Dating the appearance of Lapita pottery in the Bismarck Archipelago and its dispersal to Remote Oceania, *Archaeology in Oceania* 47(1), 39–46.

Denniston, R.F., M. DuPree, J.A. Dorale, Y. Asmerom, V.J. Polyak & S.J. Carpenter, 2007. Episodes of late Holocene aridity recorded by stalagmites from Devil's Icebox Cave, central Missouri, USA, *Quaternary Research* 68(1), 45–52.

Denniston, R.F. & M. Luetscher, 2017. Speleothems as high-resolution paleoflood archives, *Quaternary science reviews* 170, 1–13.

Dickinson, W.R., 2007. Paleoenvironment of Lapita sites on Fanga 'Uta Lagoon, Tongatapu, Kingdom of Tonga, in *Oceanic Explorations: Lapita and Western Pacific Settlement*, eds. S. Bedford, C. Sand & S.P. Connaughton (Terra Australis). : ANU Press.

Dickinson, W.R., D.V. Burley & Richard Shutler Jr., 1999. Holocene Paleoshoreline Record in Tonga: Geomorphic Features and Archaeological Implications, *Journal of Coastal Research* 15(3), 682–700.

Egli, R., 2004. Characterization of Individual Rock Magnetic Components by Analysis of Remanence Curves, 1. Unmixing Natural Sediments, *Studia Geophysica et Geodaetica* 48(2), 391–446.

Ellison, J.C., 1989. Pollen analysis of mangrove sediments as a sea-level indicator: assessment from Tongatapu, Tonga, *Palaeogeography, palaeoclimatology, palaeoecology* 74(3), 327–41.

Fairchild, I.J. & A. Baker, 2012a. Geochemistry of Speleothems, in *Speleothem Science*. : John Wiley & Sons, Ltd, 245–89.

Fairchild, I.J. & A. Baker, 2012b. *Speleothem Science : From Process to Past Environments*. Oxford [u.a.]: Blackwell.

Fassbinder, J.W.E., 2015. Seeing beneath the farmland, steppe and desert soil: magnetic prospecting and soil magnetism, *Journal of archaeological science* 56, 85–95.

Feinberg, J.M., I. Lascu, E.A. Lima, B.P. Weiss, J.A. Dorale, E.C. Alexander & R.L. Edwards, 2020. Magnetic detection of paleoflood layers in stalagmites and implications for historical land use changes, *Earth and planetary science letters* 530, 115946.

Fenner, J.N., E. Herrscher, F. Valentin & G. Clark, 2021. An isotopic analysis of Late Lapita and State Period diets in Tonga, *Archaeological and anthropological sciences* 13(1), 22.

Font, E., C. Veiga-Pires, M. Pozo, C. Carvallo, A.C. de Siqueira Neto, P. Camps, S. Fabre & J. Mirão, 2014. Magnetic fingerprint of southern Portuguese speleothems and implications for paleomagnetism and environmental magnetism: Magnetic fingerprint of speleothems, *Journal of Geophysical Research, [Solid Earth]* 119(11), 7993–8020.

Fritz, H.M., J.C. Borrero, C.E. Synolakis, E.A. Okal, R. Weiss, V.V. Titov, B.E. Jaffe, S. Foteinis, P.J. Lynett, I.-C. Chan & P.L.-F. Liu, 2011. Insights on the 2009 South Pacific tsunami in Samoa and Tonga from field surveys and numerical simulations, *Earth-Science Reviews* 107(1), 66–75.

Fukao, Y. & M. Obayashi, 2013. Subducted slabs stagnant above, penetrating through, and trapped below the 660 km discontinuity: SUBDUCTED SLABS IN THE TRANSITION ZONE, *Journal of Geophysical Research, [Solid Earth]* 118(11), 5920–38.

Fukuyo, N., G. Clark, A. Purcell, P. Parton & Y. Yokoyama, 2020. Holocene sea level reconstruction using lagoon specific local marine reservoir effect and geophysical modeling in Tongatapu, Kingdom of Tonga, *Quaternary science reviews* 244, 106464.

Fukuyo, N., Y. Yokoyama, Y. Miyairi & Y. Igarashi, 2019. AMS Dating of Potentially the Oldest Wooden Sculptures in Japan from a Shinto Shrine in Akita, *Radiocarbon* 61(5), 1221–28.

Garschagen, M., P. Mucke, A. Schauber, T. Seibert, T. Welle, J. Birkmann & J. Rhyner, 2014. World risk report, *B ündnis entwicklung hilft (alliance development works), United Nations University--Institute for Environment and Human Security (UNU-EHS), Berlin* 12–17.

Genty, D., D. Blamart, B. Ghaleb, V. Plagnes, C. Causse, M. Bakalowicz, K. Zouari, N. Chkir, J. Hellstrom & K. Wainer, 2006. Timing and dynamics of the last deglaciation from European and North African δ13C stalagmite profiles—comparison with Chinese and South Hemisphere stalagmites, *Quaternary science reviews* 25(17–18), 2118–42.

Gillikin, D.P., A. Lorrain, J. Navez, J.W. Taylor, L. André, E. Keppens, W. Baeyens & F. Dehairs, 2005. Strong biological controls on Sr/Ca ratios in aragonitic marine bivalve shells, *Geochemistry, Geophysics, Geosystems* 6(5), Q05009.

Goodwin, I.D., S.A. Browning & A.J. Anderson, 2014. Climate windows for Polynesian voyaging to New Zealand and Easter Island, *Proceedings of the National Academy of Sciences of the United States of America* 111(41), 14716–21.

Gordillo, S., M.S. Bayer, G. Boretto & M. Charó, 2014. Stable Isotopes, in *Mollusk Shells as Bio-Geo-Archives: Evaluating Environmental Changes during the Quaternary* (SpringerBriefs in Earth System Sciences). : Springer, Cham, 65–70.

Griffiths, M.L., J. Fohlmeister, R.N. Drysdale, Q. Hua, K.R. Johnson, J.C. Hellstrom, M.K. Gagan & J.-X. Zhao, 2012. Hydrological control of the dead carbon fraction in a Holocene tropical speleothem, *Quaternary geochronology* 14, 81–93.

Guyodo, Y., T.M. LaPara, A.J. Anschutz, R.L. Penn, S.K. Banerjee, C.E. Geiss & W. Zanner, 2006. Rock magnetic, chemical and bacterial community analysis of a modern soil from Nebraska, *Earth and planetary science letters* 251(1), 168–78.

Hanesch, M., H. Stanjek & N. Petersen, 2006. Thermomagnetic measurements of soil iron minerals: the role of organic carbon, *Geophysical Journal International* 165(1), 53–61.

Harrison, R.J. & J.M. Feinberg, 2008. FORCinel: An improved algorithm for calculating first-order reversal curve distributions using locally weighted regression smoothing: FORCINEL ALGORITHM, *Geochemistry, Geophysics, Geosystems* 9(5), .

Harrison, R.J., J. Muraszko, D. Heslop, I. Lascu, A.R. Muxworthy & A.P. Roberts, 2018. An Improved Algorithm for Unmixing First-Order Reversal Curve Diagrams Using Principal Component Analysis, *Geochemistry, Geophysics, Geosystems* 19(5), 1595–1610.

He, K. & Y. Pan, 2020. Magnetofossil Abundance and Diversity as Paleoenvironmental Proxies: A Case Study From Southwest Iberian Margin Sediments, *Geophysical research letters* 47(8), e2020GL087165.

Heaton, T.J., P. Köhler, M. Butzin, E. Bard, R.W. Reimer, W.E.N. Austin, C.B. Ramsey, P.M. Grootes, K.A. Hughen, B. Kromer, P.J. Reimer, J. Adkins, A. Burke, M.S. Cook, J. Olsen & L.C. Skinner, 2020. Marine20—The Marine Radiocarbon Age Calibration Curve (0–55,000 cal BP), *Radiocarbon* 62(4), 779–820.

Herath, D., D.E. Jacob, H. Jones & S.J. Fallon, 2019. Potential of shells of three species of eastern Australian freshwater mussels (Bivalvia: Hyriidae) as environmental proxy archives, *Marine and Freshwater Research* 70(2), 255–69.

Herrscher, E., J.N. Fenner, F. Valentin, G. Clark, C. Reepmeyer, L. Bouffandeau & G. André, 2018. Multi-isotopic analysis of first Polynesian diet (Talasiu, Tongatapu, Kingdom of Tonga), *Journal of Archaeological Science: Reports* 18, 308–17.

Hirabayashi, S., Y. Yokoyama, A. Suzuki, T. Esat, Y. Miyairi, T. Aze, F. Siringan & Y. Maeda, 2019. Local marine reservoir age variability at Luzon Strait in the South China Sea during the Holocene, *Nuclear instruments & methods in physics research. Section B, Beam interactions with materials and atoms*.

Hirabayashi, S., Y. Yokoyama, A. Suzuki, Y. Miyairi & T. Aze, 2017. Short-term fluctuations in regional radiocarbon reservoir age recorded in coral skeletons from the Ryukyu Islands in the north-western Pacific: SHORT-TERM FLUCTUATIONS IN LOCAL RESERVOIR AGE IN THE RYUKYUS, *Journal of Quaternary Science* 32(1), 1–6.

Hogg, A.G., T.J. Heaton, Q. Hua, J.G. Palmer, C.S.M. Turney, J. Southon, A. Bayliss, P.G. Blackwell, G. Boswijk, C.B. Ramsey, C. Pearson, F. Petchey, P. Reimer, R. Reimer & L. Wacker, 2020. SHCal20 Southern Hemisphere Calibration, 0–55,000 Years cal BP, *Radiocarbon* 62(4), 759–78.

Hogg, A.G. & T.F.G. Higham, 1998. ^{14}C DATING OF MODERN MARINE AND ESTUARINE SHELLFISH, *Radiocarbon* 40(2),

Humblet, M., D.C. Potts, J.M. Webster, J.C. Braga, Y. Iryu, Y. Yokoyama, R. Bourillot, C. Séard, A. Droxler, K. Fujita, E. Gischler & H. Kan, 2019. Late glacial to deglacial variation of coralgal assemblages in the Great Barrier Reef, Australia, *Global and planetary change* 174, 70–91.

Hunt, B., 1979. An analysis of the groundwater resources of Tongatapu Island, Kingdom of Tonga, *Journal of Hydrology* 40(1), 185–96.

Intergovernmental Panel on Climate Change, 2014. *Climate Change 2013: The Physical Science Basis: Working Group I Contribution to the Fifth Assessment Report of the Intergovernmental Panel on Climate Change*. : Cambridge University Press.

Irwin, G., T.H. Worthy, S. Best, S. Hawkins, J. Carpenter & S. Matararaba, 2011. Further Investigations at the Naigani Lapita site (VL 21/5), Fiji: Excavation, Radiocarbon Dating and Palaeofaunal Extinction, *Journal of Pacific Archaeology* 2(2), 66–78.

Jackson, K.L., G.P. Eberli, F. Amelung, M.A. McFadden, A.L. Moore, E.C. Rankey & H.A.H. Jayasena, 2014. Holocene Indian Ocean tsunami history in Sri Lanka, *Geology* 42(10), 859–62.

Jagadis, I. & S. Rajagopal, 2007. Reproductive biology of Venus clam Gafrarium tumidum (Roding, 1798) from Southeast coast of India, *Aquaculture research* 38(11), 1117–22.

Jaqueto, P., R.I.F. Trindade, G.A. Hartmann, V.F. Novello, F.W. Cruz, I. Karmann, B.E. Strauss & J.M. Feinberg, 2016. Linking speleothem and soil magnetism in the Pau d'Alho cave (central South America), *Journal of Geophysical Research, [Solid Earth]* 121(10), 7024–39.

Johnston, P., 1993. The effect of spatially non-uniform water loads on prediction of sea-level change, *Geophysical Journal International* 114(3), 615–34.

Kawai, J., H. Oda, J. Fujihira, M. Miyamoto, I. Miyagi & M. Sato, 2016. SQUID Microscope With Hollow-Structured Cryostat for Magnetic Field Imaging of Room Temperature Samples, *IEEE Transactions on Applied Superconductivity* 26(5), 1–5.

Kayanne, H., T. Yasukochi, T. Yamaguchi, H. Yamano & M. Yoneda, 2011. Rapid settlement of Majuro Atoll, central Pacific, following its emergence at 2000 years CalBP: RAPID SETTLEMENT OF ATOLL, *Geophysical research letters* 38(20) .

Kelemen, Z., D.P. Gillikin, L.E. Graniero, H. Havel, F. Darchambeau, A.V. Borges, A. Yambélé, A. Bassirou & S. Bouillon, 2017. Calibration of hydroclimate proxies in

freshwater bivalve shells from Central and West Africa, *Geochimica et cosmochimica acta* 208, 41–62.

Kench, P.S., R.F. McLean, S.D. Owen, E. Ryan, K.M. Morgan, L. Ke, X. Wang & K. Roy, 2020. Climate-forced sea-level lowstands in the Indian Ocean during the last two millennia, *Nature geoscience* 13(1), 61–64.

Kim, S.-T., A. Mucci & B.E. Taylor, 2007. Phosphoric acid fractionation factors for calcite and aragonite between 25 and 75 °C: Revisited, *Chemical geology* 246(3–4), 135–46.

Klemas, V., 2011. Remote Sensing of Sea Surface Salinity: An Overview with Case Studies, *Journal of Coastal Research* 27(5), 830–38.

Kubota, K., K. Shirai, N. Murakami-Sugihara, K. Seike, M. Minami, T. Nakamura & K. Tanabe, 2018. Bomb- ^{14} C Peak in the North Pacific Recorded in Long-Lived Bivalve Shells (Mercenaria stimpsoni), *Journal of Geophysical Research, C: Oceans* 123(4), 2867–81.

Kumar, R., P.D. Nunn, J.S. Field & A. de Biran, 2006. Human responses to climate change around AD 1300: A case study of the Sigatoka Valley, Viti Levu Island, Fiji, *Quaternary international: the journal of the International Union for Quaternary Research* 151(1), 133–43.

Lambeck, K., 2002. Sea Level Change From Mid Holocene to Recent Time: An Australian Example with Global Implications, in *Ice Sheets, Sea Level and the Dynamic Earth*, eds. J. Mitrovica & B. Vermeersen (Geodynamics Series).

Lambeck, K., A. Purcell, P. Johnston, M. Nakada & Y. Yokoyama, 2003. Water-load definition in the glacio-hydro-isostatic sea-level equation, *Quaternary science reviews* 22(2), 309–18.

Lambeck, K., A. Purcell, J. Zhao & N.-O. Svensson, 2010. The Scandinavian Ice Sheet: from MIS 4 to the end of the Last Glacial Maximum, *Boreas* 39(2), 410–35.

Lambeck, K., A. Purcell & S. Zhao, 2017. The North American Late Wisconsin ice sheet and mantle viscosity from glacial rebound analyses, *Quaternary science reviews* 158, 172–210.

Lambeck, K., H. Rouby, A. Purcell, Y. Sun & M. Sambridge, 2014. Sea level and global ice volumes from the Last Glacial Maximum to the Holocene, *Proceedings of the National Academy of Sciences of the United States of America* 111(43), 15296–303.

Lascu, I., J.F. Einsle, M.R. Ball & R.J. Harrison, 2018. The Vortex State in Geologic Materials: A Micromagnetic Perspective, *Journal of Geophysical Research, [Solid Earth]* 123(9), 7285–7304.

Lascu, I. & J.M. Feinberg, 2011. Speleothem magnetism, *Quaternary science reviews* 30(23), 3306–20.

Lascu, I., J.M. Feinberg, J.A. Dorale, H. Cheng & R. Lawrence Edwards, 2016. Age of the Laschamp excursion determined by U-Th dating of a speleothem geomagnetic record from North America, *Geology* 44(2), 139–42.

Latham, A.G., H.P. Schwarcz, D.C. Ford & G.W. Pearce, 1979. Palaeomagnetism of stalagmite deposits, *Nature* 280(5721), 383–85.

Lay, T., C.J. Ammon, H. Kanamori, L. Rivera, K.D. Koper & A.R. Hutko, 2010. The 2009 Samoa-Tonga great earthquake triggered doublet, *Nature* 466(7309), 964–68.

Lea, D.W., 2003. 6.14 - Elemental and Isotopic Proxies of Past Ocean Temperatures, in *Treatise on Geochemistry*, eds. H.D. Holland & K.K. Turekian. Oxford: Pergamon, 1–26.

Lechleitner, F.A., J. Fohlmeister, C. McIntyre, L.M. Baldini, R.A. Jamieson, H. Hercman, M. Gąsiorowski, J. Pawlak, K. Stefaniak, P. Socha, T.I. Eglinton & J.U.L. Baldini, 2016. A novel approach for construction of radiocarbon-based chronologies for speleothems, *Quaternary geochronology* 35, 54–66.

Lewis, E.R. & D.W.R. Wallace, 1998.

Li, H.-C., M. Zhao, C.-H. Tsai, H.-S. Mii, Q. Chang & K.-Y. Wei, 2015. The first high-resolution stalagmite record from Taiwan: Climate and environmental changes during the past 1300 years, *Journal of Asian Earth Sciences* 114, 574–87.

Li, S., J. Fukuda & O. Oncken, 2020. Geodetic Evidence of Time-Dependent Viscoelastic Interseismic Deformation Driven by Megathrust Locking in the Southwest Japan Subduction Zone, *Geophysical research letters* 47(4), 1135.

Li, S., K. Wang, Y. Wang, Y. Jiang & S.E. Dosso, 2018. Geodetically Inferred Locking State of the Cascadia Megathrust Based on a Viscoelastic Earth Model, *Journal of Geophysical Research, [Solid Earth]* 123(9), 8056–72.

Lima, E.A. & B.P. Weiss, 2016. Ultra-high sensitivity moment magnetometry of geological samples using magnetic microscopy: ULTRA-SENSITIVE MOMENT MAGNETOMETRY, *Geochemistry, Geophysics, Geosystems* 17(9), 3754–74.

Lindauer, S., S. Marali, B.R. Schöne, H.-P. Uerpmann, B. Kromer & M. Hinderer, 2017a. Investigating the Local Reservoir Age and Stable Isotopes of Shells from Southeast Arabia, *Radiocarbon* 59(2), 355–72.

Lindauer, S., G.M. Santos, A. Steinhof, E. Yousif, C. Phillips, S.A. Jasim, H.-P. Uerpmann & M. Hinderer, 2017b. The local marine reservoir effect at Kalba (UAE) between the Neolithic and Bronze Age: An indicator of sea level and climate changes, *Quaternary geochronology* 42, 105–16.

Linsley, B.K., A. Kaplan, Y. Gouriou, J. Salinger, P.B. deMenocal, G.M. Wellington & S.S. Howe, 2006. Tracking the extent of the South Pacific Convergence Zone since the early 1600s, *Geochemistry, Geophysics, Geosystems* 7(5), Q05003.

Liu, Q., V. Barrón, J. Torrent, H. Qin & Y. Yu, 2010. The magnetism of micro-sized hematite explained, *Physics of the Earth and Planetary Interiors* 183(3), 387–97.

Maes, C., B. Dewitte, J. Sudre, V. Garçon & D. Varillon, 2013. Small-scale features of temperature and salinity surface fields in the Coral Sea: Small-Scale Features in the Coral Sea, *Journal of Geophysical Research, C: Oceans* 118(10), 5426–38.

Mannino, M.A. & K.D. Thomas, 2002. Depletion of a resource? The impact of prehistoric human foraging on intertidal mollusc communities and its significance for human settlement, mobility and dispersal, *World archaeology* 33(3), 452–74.

Manu, V., A. Whitbread, N. Blair & G. Blair, 2014. Carbon status and structural stability of soils from differing land use systems in the Kingdom of Tonga, *Soil Use and Management* 30(4), 517–23.

Markulin, K., M. Peharda, R. Mertz-Kraus, B.R. Schöne, H. Uvanović, Ž. Kovač & I. Janeković, 2019. Trace and minor element records in aragonitic bivalve shells as environmental proxies, *Chemical geology* 507, 120–33.

Marmet, E., M. Bina, N. Fedoroff & A. Tabbagh, 1999. Relationships between human activity and the magnetic properties of soils: a case study in the medieval site of Roissy-en-France, *Archaeological Prospection* 6(3), 161–70.

Martindale, A., G.T. Cook, I. McKechnie, K. Edinborough, I. Hutchinson, M. Eldridge, K. Supernant & K.M. Ames, 2018. ESTIMATING MARINE RESERVOIR EFFECTS IN ARCHAEOLOGICAL CHRONOLOGIES: COMPARING ΔR CALCULATIONS IN PRINCE RUPERT HARBOUR, BRITISH COLUMBIA, CANADA, *American antiquity* 83(4), 659–80.

Maxbauer, D.P., J.M. Feinberg & D.L. Fox, 2016. MAX UnMix: A web application for unmixing magnetic coercivity distributions, *Computers & geosciences* 95, 140–45.

Maxbauer, D.P., J.M. Feinberg, D.L. Fox & E.A. Nater, 2017. Response of pedogenic magnetite to changing vegetation in soils developed under uniform climate, topography, and parent material, *Scientific reports* 7(1), 17575.

Mcmahon, R.F., 2003. Contributions of the Hong Kong malacological and marine workshops to the comparative and ecological physiology of intertidal invertebrates, in *Perspectives on Marine Environmental Change in Hong Kong, 1977-2001*, ed. B. Morton. : Hong Kong University Press, HKU, 479–515.

Meffre, S., T.J. Falloon, T.J. Crawford, K. Hoernle, F. Hauff, R.A. Duncan, S.H. Bloomer & D.J. Wright, 2012. Basalts erupted along the Tongan fore arc during subduction initiation: Evidence from geochronology of dredged rocks from the Tonga fore arc and trench: TONGA FORE ARC, *Geochemistry, Geophysics, Geosystems* 13(12).

Mitrovica, J.X. & G.A. Milne, 2002. On the origin of late Holocene sea-level highstands within equatorial ocean basins, *Quaternary science reviews* 21(20), 2179–90.

Morinaga, H., H. Inokuchi & K. Yaskawa, 1989. Palaeomagnetism of stalagmites (speleothems) in SW Japan, *Geophysical Journal International* 96(3), 519–28.

Myre, J.M., I. Lascu, E.A. Lima, J.M. Feinberg, M.O. Saar & B.P. Weiss, 2019. Using TNT-NN to unlock the fast full spatial inversion of large magnetic microscopy data sets, *Earth, Planets and Space* 71(1), 14.

Nakada, M. & K. Lambeck, 1987. Glacial rebound and relative sea-level variations: a new appraisal, *Geophysical journal international* 90(1), 171–224.

Nishida, K., Y.C. Chew, Y. Miyairi, S. Hirabayashi, A. Suzuki, M. Hayashi, Y. Yamamoto, M. Sato, Y. Nojiri & Y. Yokoyama, 2020. Novel reverse radioisotope labelling experiment reveals carbon assimilation of marine calcifiers under ocean acidification conditions, (ed.)Trueman, C. *Methods in ecology and evolution / British Ecological Society* 11(6), 739–50.

Noguchi, A., H. Oda, Y. Yamamoto, A. Usui, M. Sato & J. Kawai, 2017. Scanning SQUID microscopy of a ferromanganese crust from the northwestern Pacific: Submillimeter scale magnetostratigraphy as a new tool for age determination and mapping of environmental magnetic parameters: SQUID Microscopy of Ferromanganese Crust, *Geophysical research letters* 44(11), 5360–67.

Nunn, P.D. & M.T. Carson, 2015. Sea-level fall implicated in profound societal change about 2570 cal yr bp (620 bc) in western Pacific island groups : Sea-level fall implicated in profound societal change in western Pacific island groups, *Geo: Geography and Environment* 2(1), 17–32.

Oda, H., J. Kawai, M. Miyamoto, I. Miyagi, M. Sato, A. Noguchi, Y. Yamamoto, J.-I. Fujihira, N. Natsuhara, Y. Aramaki, T. Masuda & C. Xuan, 2016. Scanning SQUID microscope system for geological samples: system integration and initial evaluation, *Earth, Planets and Space* 68(1), 179.

Oda, H., J. Kawai, A. Usui, Y. Yamamoto, A. Noguchi, I. Miyagi, M. Miyamoto, J. Fujihira & M. Sato, 2020. Development of scanning SQUID microscope system and its applications on geological samples: A case study on marine ferromanganese crust, *Journal of physics. Conference series* 1590(1), 012037.

Openshaw, S., A. Latham & J. Shaw, 1997. Speleothem Palaeosecular Variation Records from China: Their Contribution to the Coverage of Holocene Palaeosecular Variation Data in East Asia, *Journal of geomagnetism and geoelectricity* 49(4), 485–505.

Osete, M.-L., J. Martín-Chivelet, C. Rossi, R.L. Edwards, R. Egli, M.B. Muñoz-García, X. Wang, F.J. Pavón-Carrasco & F. Heller, 2012. The Blake geomagnetic excursion recorded in a radiometrically dated speleothem, *Earth and planetary science letters* 353–354, 173–81.

Paterson, G.A., X. Zhao, M. Jackson & D. Heslop, 2018. Measuring, Processing, and Analyzing Hysteresis Data, *Geochemistry, Geophysics, Geosystems* 19(7), 1925–45.

Petchey, F., 2020. NEW EVIDENCE FOR A MID- TO LATE-HOLOCENE CHANGE IN THE MARINE RESERVOIR EFFECT ACROSS THE SOUTH PACIFIC GYRE, *Radiocarbon* 1–13.

Petchey, F., A. Anderson, A. Hogg & A. Zondervan, 2008. The marine reservoir effect in the Southern Ocean: An evaluation of extant and new ΔR values and their application to archaeological chronologies, *Journal of the Royal Society of New Zealand* 38(4), 243–62.

Petchey, F. & G. Clark, 2011. Tongatapu hardwater: Investigation into the ^{14}C marine reservoir offset in lagoon, reef and open ocean environments of a limestone island, *Quaternary geochronology* 6(6), 539–49.

Petchey, F., S. Ulm, B. David, I.J. McNiven, B. Asmussen, H. Tomkins, N. Dolby, K. Aplin, T. Richards, C. Rowe & Others, 2013. High-resolution radiocarbon dating of marine materials in archaeological contexts: radiocarbon marine reservoir variability between Anadara, Gafrarium, Batissa, Polymesoda spp. and Echinoidea at Caution Bay, Southern Coastal Papua New Guinea, *Archaeological and anthropological sciences* 5(1), 69–80.

Ponte, J.M., E. Font, C. Veiga-Pires & C. Hillaire-Marcel, 2018. Speleothems as Magnetic Archives: Paleosecular Variation and a Relative Paleointensity Record From a Portuguese Speleothem, *Geochemistry, Geophysics, Geosystems* 19(9), 2962–72.

Poulain, C., D.P. Gillikin, J. Thébault, J.M. Munaron, M. Bohn, R. Robert, Y.-M. Paulet & A. Lorrain, 2015. An evaluation of Mg/Ca, Sr/Ca, and Ba/Ca ratios as environmental proxies in aragonite bivalve shells, *Chemical geology* 396, 42–50.

Pozzi, J.-P., L. Rousseau, C. Falguères, G. Mahieux, P. Deschamps, Q. Shao, D. Kachi, J.-J. Bahain & C. Tozzi, 2019. U-Th dated speleothem recorded geomagnetic excursions in the Lower Brunhes, *Scientific reports* 9(1), 1114.

Ramsey, C.B., 2008. Deposition models for chronological records, *Quaternary science reviews* 27(1), 42–60.

Ramsey, C.B., 2009a. Bayesian Analysis of Radiocarbon Dates, *Radiocarbon* 51(1), 337–60.

Ramsey, C.B., 2009b. Dealing with Outliers and Offsets in Radiocarbon Dating, *Radiocarbon* 51(3), 1023–45.

Ramsey, C.B. & S. Lee, 2013. Recent and Planned Developments of the Program OxCal, *Radiocarbon* 55(2–3), 720–30.

Reimer, P.J., R.W. Reimer & M. Blaauw, 2013. RADIOCARBON DATING | Calibration of the ^{14}C Record, in *Encyclopedia of Quaternary Science (Second Edition)*, eds. S.A. Elias & C.J. Mock. Amsterdam: Elsevier, 345–52.

Reimer, R.W. & P.J. Reimer, 2017. An Online Application for ΔR Calculation, *Radiocarbon* 59(5), 1623–27.

Roberts, A.P., F. Florindo, L. Chang, D. Heslop, L. Jovane & J.C. Larrasoaña, 2013. Magnetic properties of pelagic marine carbonates, *Earth-Science Reviews* 127, 111–39.

Roberts, A.P., D. Heslop, X. Zhao & C.R. Pike, 2014. Understanding fine magnetic particle systems through use of first-order reversal curve diagrams, *Reviews of geophysics* 52(4), 2014RG000462.

Rosenthal, Y. & B. Linsley, 2007. PALEOCEANOGRAPHY, PHYSICAL AND CHEMICAL PROXIES | Mg/Ca and Sr/Ca Paleothermometry, in *Encyclopedia of Quaternary Science*, ed. S.A. Elias. Oxford: Elsevier, 1723–31.

Roy, P.S., 1997. The morphology and surface geology of the islands of Tongatapu and Vava'u, Kingdom of Tonga, in *Coastal and Environmental Geoscience Studies of the Southwest Pacific Islands*, eds. M.S. Alan, H. Russell & R. Peter. : SOPAC Secretariat, 153–73.

Rull, V., N. Cañellas-Boltà, O. Margalef, A. Sáez, S. Pla-Rabes & S. Giralt, 2015. Late Holocene vegetation dynamics and deforestation in Rano Aroi: Implications for Easter Island's ecological and cultural history, *Quaternary science reviews* 126, 219–26.

Sawkins, J.G., 1856. On the Movement of Land in the South Sea Islands, *Quarterly Journal of the Geological Society of London* 12(1–2), 383–84.

Schroeder, H., T.C. O'Connell, J.A. Evans, K.A. Shuler & R.E.M. Hedges, 2009. Trans-Atlantic slavery: isotopic evidence for forced migration to Barbados, *American journal of physical anthropology* 139(4), 547–57.

Schwarcz, H., 2013. CARBONATE STABLE ISOTOPES | Speleothems, in *Encyclopedia of Quaternary Science (Second Edition)*, eds. S.A. Elias & C.J. Mock. Amsterdam: Elsevier, 294–303.

Shirai, K., F. Koyama, N. Murakami-Sugihara, K. Nanjo, T. Higuchi, H. Kohno, Y. Wananabe, K. Okamoto & M. Sano, 2018. Reconstruction of the salinity history associated with movements of mangrove fishes using otolith oxygen isotopic analysis, *Marine ecology progress series* 593, 127–39.

Spennemann, D.H.R., 1987. Availability of Shellfish Resources on Prehistoric Tongatapu, Tonga: Effects of Human Predation and Changing Environment, *Archaeology in Oceania* 22(3), 81–96.

Spennemann, D.H.R., 1997. A Holocene sea-level history for Tongatapu, Kingdom of Tonga, *Coastal and Environmental geoscience studies of the Southwest Pacific Islands. SOPA Technical Bulletin* 9, 115–52.

Spennemann, D.H.R. & M. John Head, 1998. Tongan pottery chronology, ^{14}C dates and the hardwater effect, *Quaternary science reviews* 17(11), 1047–56.

Spennemann, D.R., 1989. *'Ata 'a Tonga Mo 'Ata 'o Tonga : Early and Later Prehistory of the Tongan Islands*, The Australian National University.

Stott, L., K. Cannariato, R. Thunell, G.H. Haug, A. Koutavas & S. Lund, 2004. Decline of surface temperature and salinity in the western tropical Pacific Ocean in the Holocene epoch, *Nature* 431(7004), 56–59.

Strauss, B.E., J.H. Strehlau, I. Lascu, J.A. Dorale, R.L. Penn & J.M. Feinberg, 2013. The origin of magnetic remanence in stalagmites: Observations from electron microscopy and rock magnetism, *Geochemistry, Geophysics, Geosystems* 14(12), 5006–25.

Stuiver, M. & H.A. Polach, 1977. Discussion Reporting of ^{14}C Data, *Radiocarbon* 19(3), 355–63.

Tang, L., V.V. Titov, Y. Wei, H.O. Mofjeld, M. Spillane, D. Arcas, E.N. Bernard, C. Chamberlin, E. Gica & J. Newman, 2008. Tsunami forecast analysis for the May 2006 Tonga tsunami: FORECAST ANALYSIS FOR THE 2006 TONGA TSUNAMI, *Journal of geophysical research* 113(C12), .

Taylor, F.W., 1978. *Quaternary Tectonic and Sea-Level History, Tonga and Fiji, Southwest Pacific*, Cornell University.

Taylor, R.M. & U. Schwertmann, 1974. Maghemite in soils and its origin: II. Maghemite syntheses at ambient temperature and pH 7, *Clay minerals* 10(4), 299–310.

Tibi, R. & D.A. Wiens, 2005. Detailed structure and sharpness of upper mantle discontinuities in the Tonga subduction zone from regional broadband arrays, *Journal of geophysical research* 110(B6), 15,671.

van der Hilst, R., 1995. Complex morphology of subducted lithosphere in the mantle beneath the Tonga trench, *Nature* 374(6518), 154–57.

van der Velde, M., S.R. Green, G.W. Gee, M. Vanclooster & B.E. Clothier, 2005. Evaluation of Drainage from Passive Suction and Nonsuction Flux Meters in a Volcanic Clay Soil under Tropical Conditions, *Vadose Zone Journal* 4(4), 1201–9.

van der Velde, M., S.R. Green, M. Vanclooster & B.E. Clothier, 2006a. Transpiration of Squash Under a Tropical Maritime Climate, *Plant and soil* 280(1), 323–37.

van der Velde, M., M. Javaux, M. Vanclooster & B.E. Clothier, 2006b. El Niño-Southern Oscillation determines the salinity of the freshwater lens under a coral atoll in the Pacific Ocean, *Geophysical research letters* 33(21), L21403.

Van Heuven, S., D. Pierrot, J.W.B. Rae, E. Lewis & D.W.R. Wallace, 2011. MATLAB program developed for CO2 system calculations, *ORNL/CDIAC-105b. Carbon Dioxide Information Analysis Center, Oak Ridge National Laboratory, US Department of Energy, Oak Ridge, Tennessee* 530, .

Vincent, D.G., 1994. The South Pacific Convergence Zone (SPCZ): A Review, *Monthly Weather Review* 122(9), 1949–70.

Wang, K. & A.M. Tréhu, 2016. Invited review paper: Some outstanding issues in the study of great megathrust earthquakes—The Cascadia example, *Journal of Geodynamics* 98, 1–18.

Webster, J.M., J.C. Braga, M. Humblet, D.C. Potts, Y. Iryu, Y. Yokoyama, K. Fujita, R. Bourillot, T.M. Esat, S. Fallon, W.G. Thompson, A.L. Thomas, H. Kan, H.V. McGregor, G. Hinestrosa, S.P. Obrochta & B.C. Lougheed, 2018. Response of the Great Barrier Reef to sea-level and environmental changes over the past 30,000 years, *Nature geoscience* 11(6), 426–32.

Weiss, B.P., E.A. Lima, L.E. Fong & F.J. Baudenbacher, 2007. Paleomagnetic analysis using SQUID microscopy, *Journal of geophysical research* 112(B9), 11715.

White, I. & T. Falkland, 2010. Management of freshwater lenses on small Pacific islands, *Hydrogeology journal* 18(1), 227–46.

White, I., T. Falkland & T. Fatai, 2009. Vulnerability of Groundwater in Tongatapu, Kingdom of Tonga, *SOPAC/EU EDF 8 Reducing the Vulnerability of Pacific APC States.*

Widlansky, M.J., A. Timmermann, K. Stein, S. McGregor, N. Schneider, M.H. England, M. Lengaigne & W. Cai, 2013. Changes in South Pacific rainfall bands in a warming climate, *Nature climate change* 3(4), 417–23.

Woodroffe, C.D., 1983. The impact of cyclone Isaac on the coast of Tonga, *Pacific Science* 37(3), 181–210.

Woodroffe, C.D., H.V. McGregor, K. Lambeck, S.G. Smithers & D. Fink, 2012. Mid-Pacific microatolls record sea-level stability over the past 5000 yr, *Geology* 40(10), 951–54.

Yamane, M., Y. Yokoyama, S. Hirabayashi, Y. Miyairi, N. Ohkouchi & T. Aze, 2019. Small- to ultra-small-scale radiocarbon measurements using newly installed single-stage AMS at the University of Tokyo, *Nuclear instruments & methods in physics research. Section B, Beam interactions with materials and atoms* 455, 238–43.

Yokoyama, Y. & T.M. Esat, 2015. Coral reefs, in *Handbook of Sea-Level Research*, eds. I. Shennan, A.J. Long & B.P. Horton. Chichester, UK: John Wiley & Sons, Ltd, 104–24.

Yokoyama, Y., T.M. Esat, W.G. Thompson, A.L. Thomas, J.M. Webster, Y. Miyairi, C. Sawada, T. Aze, H. Matsuzaki, J. Okuno, S. Fallon, J.-C. Braga, M. Humblet, Y. Iryu, D.C. Potts, K. Fujita, A. Suzuki & H. Kan, 2018. Rapid glaciation and a two-step sea level plunge into the Last Glacial Maximum, *Nature* 559(7715), 603–7.

Yokoyama, Y., S. Hirabayashi, K. Goto, J. Okuno, A.D. Sproson, T. Haraguchi, N. Ratnayake & Y. Miyairi, 2019a. Holocene Indian Ocean sea level, Antarctic melting history and past Tsunami deposits inferred using sea level reconstructions from the Sri Lankan, Southeastern Indian and Maldivian coasts, *Quaternary science reviews* 206, 150–61.

Yokoyama, Y., M. Koizumi, H. Matsuzaki, Y. Miyairi & N. Ohkouchi, 2010. Developing Ultra Small-Scale Radiocarbon Sample Measurement at the University of Tokyo, *Radiocarbon* 52(2), 310–18.

Yokoyama, Y., Y. Maeda, J. Okuno, Y. Miyairi & T. Kosuge, 2016. Holocene Antarctic melting and lithospheric uplift history of the southern Okinawa trough inferred from mid- to late-Holocene sea level in Iriomote Island, Ryukyu, Japan, *Quaternary international: the journal of the International Union for Quaternary Research* 397(Supplement C), 342–48.

Yokoyama, Y., Y. Miyairi, T. Aze, M. Yamane, C. Sawada, Y. Ando, M. de Natris, S. Hirabayashi, T. Ishiwa, N. Sato & N. Fukuyo, 2019b. A single stage Accelerator Mass Spectrometry at the Atmosphere and Ocean Research Institute, The University of Tokyo, *Nuclear instruments & methods in physics research. Section B, Beam interactions with materials and atoms*.

Yokoyama, Y., Y. Miyairi, H. Matsuzaki & F. Tsunomori, 2007. Relation between acid dissolution time in the vacuum test tube and time required for graphitization for AMS target preparation, *Nuclear instruments & methods in physics research. Section B, Beam interactions with materials and atoms* 259(1), 330–34.

Yokoyama, Y., A. Purcell & T. Ishiwa, 2019c. Gauging Quaternary Sea Level Changes Through Scientific Ocean Drilling, *Oceanography* 32(1), 64–71.

Yoshimoto, S., S. Ishida, T. Kobayashi, K. Koda, T. Tsuchihara & K. Shirahata, 2020. Using hydrogeochemical indicators to interpret groundwater flow and geochemical evolution of a freshwater lens on Majuro Atoll, Republic of the Marshall Islands, *Hydrogeology journal* 28(3), 1053–75.

Yousefi, M., G. Milne, S. Li, K. Wang & A. Bartholet, 2020. Constraining Interseismic Deformation of the Cascadia Subduction Zone: New Insights From Estimates of Vertical Land Motion Over Different Timescales, *Journal of Geophysical Research, [Solid Earth]* 125(3), 285.

Zanella, E., E. Tema, L. Lanci, E. Regattieri, I. Isola, J.C. Hellstrom, E. Costa, G. Zanchetta, R.N. Drysdale & F. Magrì, 2018. A 10,000 yr record of high-resolution Paleosecular Variation from a flowstone of Rio Martino Cave, Northwestern Alps, Italy, *Earth and planetary science letters* 485, 32–42.

Zann, L., 1984. Corals: a clue to Fanga'uta's past, *Sea Grant Cooperative Report UNIHI-SEAGRANT-CR-84-04* 39–46.

Zann, L.P., W.J. Kimmerer & R.E. Brock, 1984. *The Ecology of Fanga'uta Lagoon, Tongatapu, Tonga*. : University of Hawaii Sea Grant Program.

Zhang, H., Y. Cai, L. Tan, H. Cheng, S. Qin, Z. An, R.L. Edwards & L. Ma, 2015. Large variations of δ13C values in stalagmites from southeastern China during historical times: implications for anthropogenic deforestation: $\delta^{13}C$ in stalagmites and anthropogenic deforestation, SE China, *Boreas* 44(3), 511–25.

Zhao, L., K. Shirai, N. Murakami-Sugihara, T. Higuchi, T.T. Sakamoto, T. Miyajima & K. Tanaka, 2019. Retrospective monitoring of salinity in coastal waters with mussel shells, *The Science of the total environment* 671, 666–75.

Zhu, Z., J.M. Feinberg, S. Xie, M.D. Bourne, C. Huang, C. Hu & H. Cheng, 2017. Holocene ENSO-related cyclic storms recorded by magnetic minerals in speleothems of central China, *Proceedings of the National Academy of Sciences of the United States of America* 114(5), 852–57.

Appendix 1: Trace element analyses

本節については、5 年以内に雑誌等で刊行予定のため、非公開。